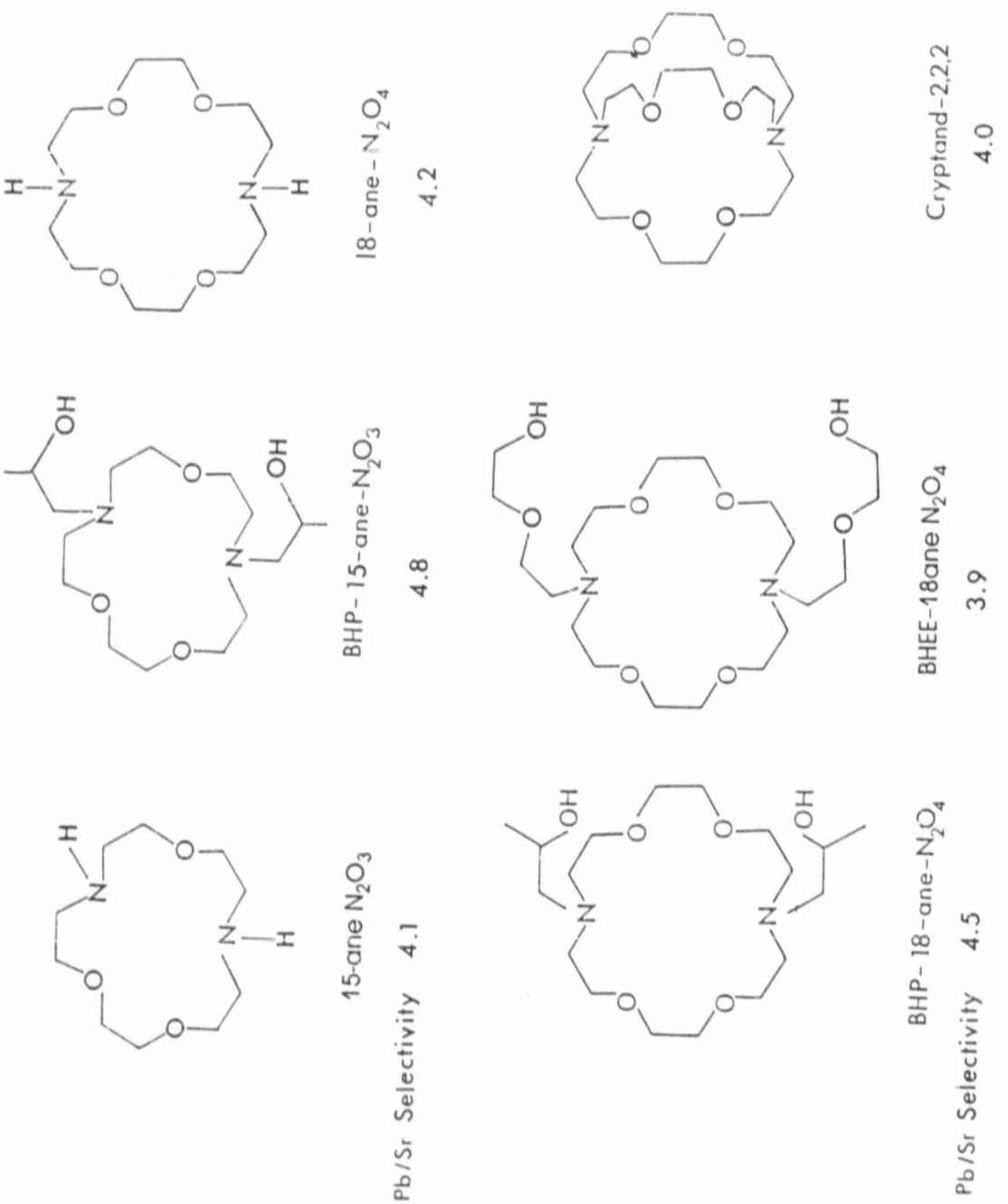

Fig. 3.3.5 The Pb^{2+}/Sr^{2+} selectivities for a series of ligands having a constant number of non–oxygen donor atoms. The Pb^{2+}/Sr^{2+} selectivity is log $K_1(Pb^{2+})$ minus log $K_1(Sr^{2+})$

strength of Pb^{2+} is by using ligands which already have high affinities for Pb^{2+}. For example, the ligand DAK–2,2, shown below, has a log K_1 value for Pb^{2+} of 14.54 log units, but the selectivity of Pb^{2+} over Zn^{2+} is low compared to that in BHEE–18–ane N_2O_4. The ligand DAK–2,2 is not sterically very demanding but can be made so by the introduction of more oxygen donor groups. Thus, if the structural complexity of BHEE–18–ane N_2O_4 is incorporated into DAK–2,2 a substantial increase in binding strength of Pb^{2+} can be achieved, as shown in Fig. 3.3.6.

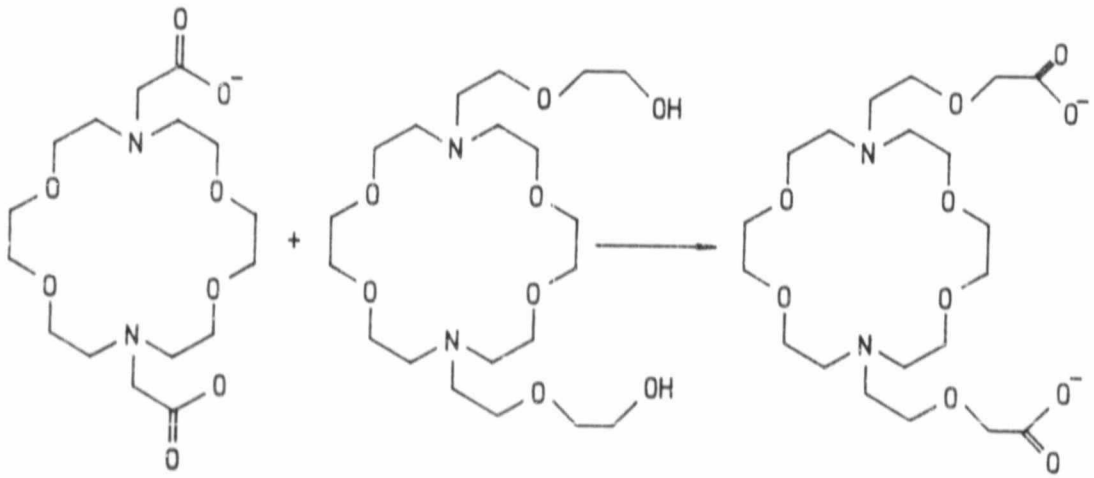

Fig. 3.3.6 A possibly way of achieving a high selectivity for Pb^{2+} over Zn^{2+} is by adding oxygen–donor bearing groups to existing ligands. The values in brackets are estimated. The selectivity, indicated as Pb^{2+}/Zn^{2+}, is log K_1 (Pb^{2+}) minus log K_1 (Zn^{2+}).

A point of interest is the origin of the metal ion size selectivity accompanying the addition of oxygen donor groups. Hancock and Martell (100) have discussed the origin of the size–selective coordinating properties in terms of the balance between steric and inductive effects when neutral oxygen donor groups coordinate to a metal ion. This idea has been supported by molecular mechanics calculations (31). These calculations indicated that in the gas phase the M–O bond strength should follow the order $Li^+ > Na^+ > K^+ > Rb^+ > Cs^+$. However, as the metal ions decrease in size, the steric crowding around the metal ion increases which leads to the reversal in stability order to give $K^+ > Na^+ > Li^+$. The stability order $K^+ > Rb^+ > Cs^+$ for 18–crown–6 reflects the intrinsic bond strength $K^+ > Rb > Cs^+$ and does not reflect a better fit of K^+ into the cavity since the strain in the Cs^+ complex of 18–crown–6 is lower than that in the K^+ complex (31). Thus, the lower stability of the Cs^+ complex is because of the lower Cs–O bond strength compared to the K–O bond strength. The same type of behaviour is found in open–chain polyethers (38) where the stability patterns are similar to those observed in crown ethers, hence supporting the idea of steric crowding being responsible for the observed size match selectivity. The same factors operate in ligands where neutral oxygen donor groups have been added. For example, for the series of ligands EN, HEEN, DHEEN and THEEN, which are derived from EN by the addition of one, two and four hydroxyethyl groups respectively (32), the change in complex stability, Δ log K, versus ionic radius is seen in Fig. 3.3.7. It is seen that there is a strong tendency for large metal ions such as Pb^{2+} and Cd^{2+} to show an increase in complex stability as more and more oxygen donors are added, whereas the smaller metal ions such as Cu^{2+} and Zn^{2+} show decreases in complex stability.

To date, all work indicates that generally only large metal ions show an increase in complex stability when groups bearing neutral oxygen donors are added to existing ligands. This may be interpreted in terms of the fact that large metal ions have high coordination numbers and are thus able to accommodate ligands with a large

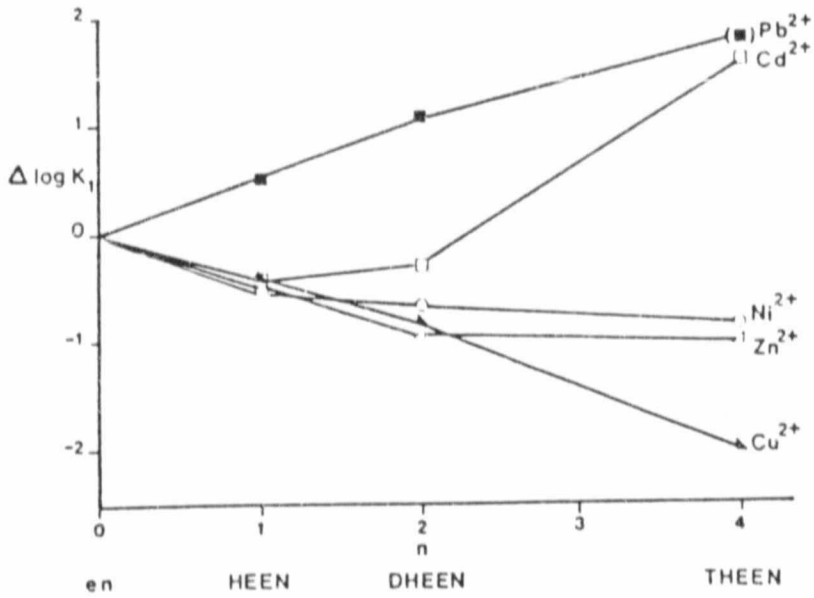

Fig. 3.3.7 The change in complex stability relative to EN as hydroxyethyl groups are added to EN to give, successively, HEEN, DHEEN, and THEEN. n is the number of hydroxyethyl groups added to EN. Reproduced with permission from Ref. 32.

number of donor atoms. On the other hand, small metal ions have lower coordination numbers and are thus unable to accommodate the large number of donor atoms in highly dendate ligands. The implication here is that in ligands which have large number of oxygen donors, the selectivity is merely an effect due to the inability of small metal ions to coordinate to all the oxygen donors, resulting in the lower complex stability. However, the metal ion size–selectivity observed in ligands containing a large number of oxygen donors is similar to that observed in ligands with one or two oxygen donors. That is, ligand systems of high denticity display selectivity patterns identical to systems of low denticity. For example, the ligand HEEN which is derived from EN by the addition of a single hydroxyethyl

group, shows a change in stability that is size selective for large metal ions. The increase in denticity in going from EN to HEEN is only from two to three which does not exceed the coordination number of any metal ions under consideration. These results appear to indicate that the effect is not simply a matter of exceeding the maximum coordination number of small metal ions since the ligand HEEN requires the metal ion to accommodate only three donor atoms.

An important factor here is the relative basicity of the donor atoms. Gas–phase studies (14) have indicated that the order of basicity increases strongly with $H_2O<ROH<R_2O$, where R = alkyl group. Since the alcoholic or ethereal oxygen donors must compete with water for coordination sites on the metal ion, and alcohols and ethers are better bases than water, an increase in complex stability for all metal ions is expected when ethereal or alcoholic oxygen donors are added to existing ligands, provided the maximum coordination number of the metal ion is not exceeded.

The origin of the metal ion size–selectivity pattern observed when neutral oxygen donors are added to a macrocycle can be understood in terms of the cyclohexane ring. The ideal geometry, which represents the minimum strain energy situation, has all the hydrogens in a staggered conformation, all tortional angles of 60°, and all bond angles of 109.5°. Any ring which comes close to this arrangement will thus be of low strain energy. As seen in Fig. 3.3.8, the six–membered chelate ring can adopt the strain free cyclohexane ring with short M–N bond lengths and large N–M–N angles. Thus, ideal geometry can be retained when a small metal ion forms part of the six–membered chelate ring. With larger metal ions, the hydrogens are forced into the less favourable eclipsed conformation. On the other hand, five–membered chelate rings retain ideal geometry with long M–N bond lengths and small N–M–N angles.

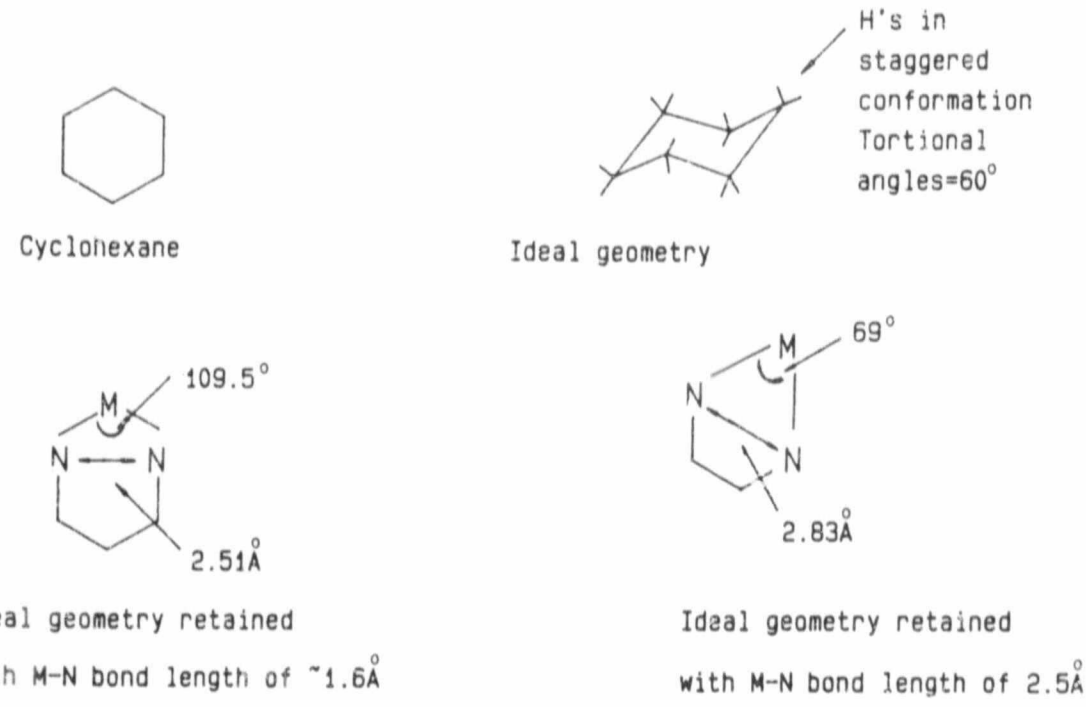

Fig. 3.3.8 Ideal geometries of the five– and six–membered chelate rings.

Thus, ideal geometry is retained when large metal ions form part of the five–membered chelate ring. As discussed in Section 1.5, for metal ion complexes that form five–membered chelate rings, the minimum strain energy is observed with M–N bond lengths of 2.5 Å and N–M–N bond angles of 69°, whereas for metal ion complexes that form six–membered chelate rings, the minimum strain energy is observed with M–N bond length of 1.6 Å and N–M–N bond angles of 109.5° (35). Thus, in five–membered chelate rings, smaller metal ions with larger N–M–N bond angles cause large rises in strain energy. Therefore, the ability of large metal ions to coordinate strongly with chelate rings containing neutral oxygen donor atoms derives from the fact that larger metal ions coordinate with less strain energy, that is, larger metal ions are better suited geometrically to coordinating to the five–membered chelate ring. Thus, for the oxygen–donor containing chelate ring the steric effects are able to predominate over the bond strength effects and a

nett destabilization of complex formation with small metal ions is observed. The reason that ligands containing the neutral oxygen donor tend to favour large metal ions is that large metal ions can coordinate from the steric point of view more satisfactorily with the five–membered chelate rings present. This is a more important factor than the cavity–size of crown ethers which never complex small metal ions well even with small cavity sizes. The effect is not readily apparent for ligands containing all nitrogen donors, such as EN or its larger homologues DIEN through PENTEN. Small metal ions such as Cu^{2+} complex well with the ligand EN which forms five–membered chelate rings. However, the strain energy effects in five–membered chelate rings whether they contain oxygen or nitrogen donors are similar. The important difference is that alcoholic and ethereal donors are only slightly better bases than the water with which they compete for coordination sites on the metal ion, while nitrogen donors are for most metal ions (100) very much better donors than is water. Thus, for the oxygen–donor chelate ring the steric effects are able to predominate over the bond strength effects whereas for nitrogen donors M–N bond formation predominates over the steric effects.

3.4 THE STRUCTURES OF THE COMPLEXES

It has been shown in the previous section that addition of pendent groups containing one or more neutral oxygen donors to a macrocycle greatly increases the level of steric crowding. Since large metal ions are able to coordinate to a large number of donor atoms, it was of interest to compare the structures of $[K(BHE–18–ane\ N_2O_4)]^+$ with that of the sterically more demanding $[K(BHEE–18–ane\ N_2O_4)]^+$.

From the structure of $[K(BHEE–18–and\ N_2O_4)]I$, it was found that the donor oxygens were not all coordinated to the K^+ cation. This was surprising, since for the Ba^{2+} ion the extra oxygens of the pendent arms produced an increase in

complex stability as compared with the DHP–18–ane N_2O_4 complex. This increase in stability would be unlikely if the extra oxygens of BHEE–18–ane N_2O_4 are non–coordinating. The Ba^{2+} and K^+ ions are similar in size (ionic radius of 1.36 and 1.38 Å for 6–coordination, respectively) (98), so that the levels of steric crowding should be similar in both the Ba^{2+} and K^+ complexes of BHEE–18–ane N_2O_4. This necessitated the structural determination of $[Ba(BHEE–18–ane\ N_2O_4)]^{2+}$ to see whether the extra oxygen donors in BHEE–18–ane N_2O_4 actually coordinate.

3.4.1 The Structure of [K(BHE–18–ane N_2O_4)]Cl

In Fig. 2.5.3a is seen the structure of the $[K(BHE–18–ane\ N_2O_4)]Cl$ complex and in Fig. 3.4.1 the skeletal diagram of the donor atoms. The skeletal diagram shows the donor atoms of the macrocycle to be arranged in a boat conformation. The metal ion is eight coordinate and is situated slightly above the plane of the macrocycle. The complex lies on a two–fold axis. The chloride anion is also situated on this axis, above but not bonded to the K^+ cation. Selected structural data are given in Table 9.

The oxygen donors of the pendent arms are closer to the metal than the macrocyclic donors. The K–N distances are substantially longer than the K–O distances suggesting that the nitrogen atoms are poorer donor atoms. The poor donor properties of the nitrogen atom relative to the oxygen atom towards alkali metal cations have been established by various workers (114,115,124). The N–M–N angle is approximately 180°. The R value is 1.46 Å and compares well with Shannon's ionic radii (98). The structure of this complex is completely analogous to the structure of $[K(BHE–18–ane\ N_2O_4)]$. I reported by Gokel et al. (113).

Table 9 Selected structural and binding parameters for [K(BHE–18–ane N_2O_4)]Cl, [K(BHEE–18–ane N_2O_4)]I and [Ba(BHEE–18–ane N_2O_4)]$I_2 \cdot 3H_2O$

Interaction	[K(BHE–18–aneN_2O_4)]Cl	[K(BHEE–18–aneN_2O_4)]I	[Ba(BHEE–18–aneN_2O_4)]I_2
M–O, Å (ring)	2.850	2.775	2.822
	2.850	2.739	2.822
	2.857	2.718	2.905
	2.857	2.849	2.905
(side–arm)	2.718	2.818	2.938
	2.718	3 192	2.938
		3.256	2.846
			2.846
(water)			2.854
M–N, Å	3.104	2.926	3.079
	3.104	2.915	3.079
N–M–N, deg	176.51	169.89	170.33
R[a], Å	1.40		1.50
major compt		1.44 (8–coord)	
		1.49 (9–coord)	
minor compt		1.39 (7–coord)	
		1.45 (8–coord)	
Coord No.	8		11
major compt		8 or 9	
minor compt		7 or 8	

[a] Mean cavity radius, as defined by Mathieu et al. (123)

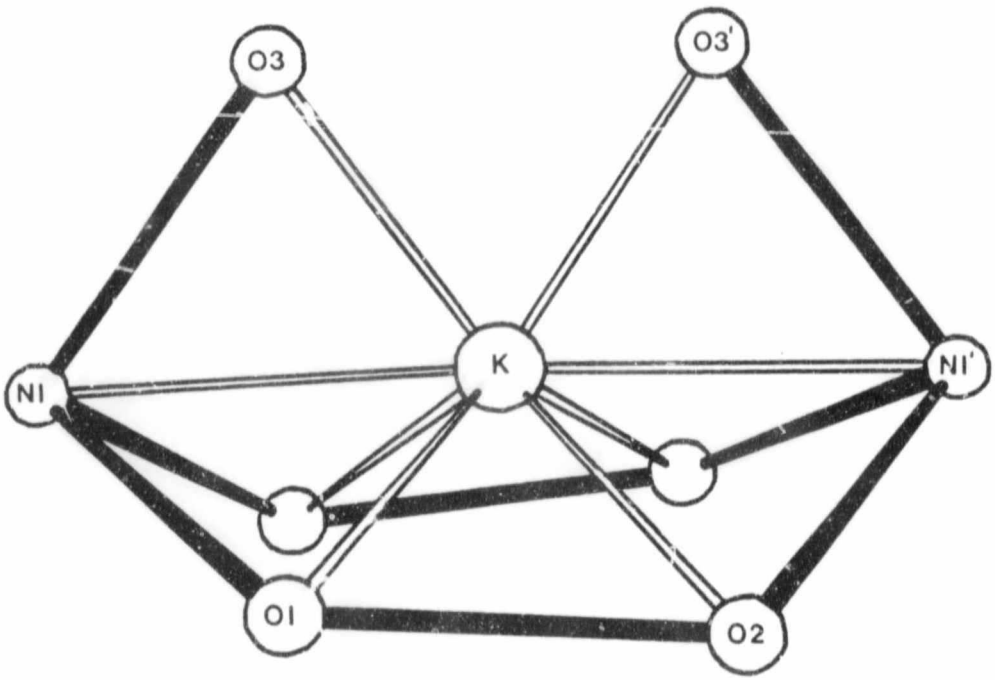

Fig. 3.4.1 Skeletal Diagram of the potassium complex of BHE–18–ane N_2O_4

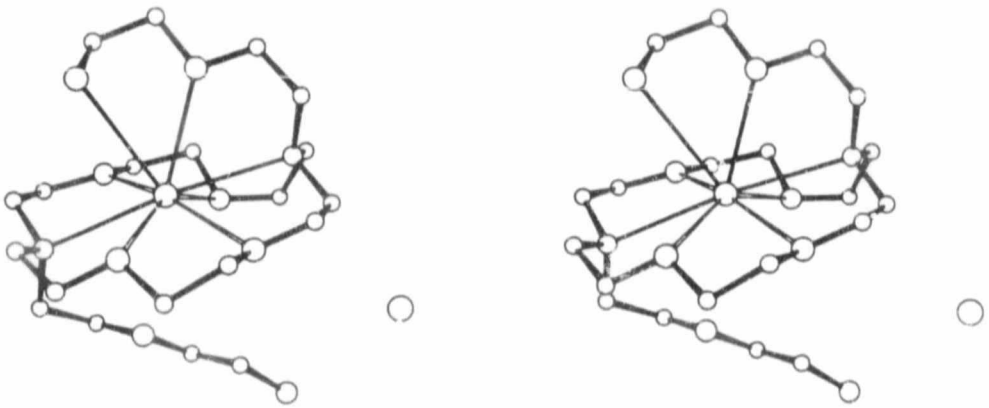

Fig. 3.4.2 Stereo view of the major conformer of [K(BHEE–18–ane N_2O_4)]$^+$

3.4.2 The structure of [K(BHEE–18–ane N_2O_4)]I

During refinement of the structure of [K(BHEE–18–ane N_2O_4)]I it became apparent that there was disorder in the terminal portion of one of the side arms, represented by the atoms C15–C16–O6. Refinement of the positions and site occupancy factors (SOF) for this disordered fragment indicated the two alternative orientations for C15–C16–O6 [SOF = 0.75(1)] and C15'–C16'–O6' [SOF = 0.25(1)], shown in Fig. 2.5.3c,d. The two disordered individuals differ only in that in the major form the terminal 06 is coordinated to the metal ion, whereas in the minor form it is not. The hydrogen of 06 is hydrogen bonded to an iodide in the same unit cell, whereas that of 06' is hydrogen bonded to an iodide in a neighbouring unit cell. The structure and numbering scheme of the two disordered individuals are shown in Fig. 2.5.3c,d. In Fig. 3.4.2 is seen a stereo view of the major conformer and in Fig. 3.4.3 are seen the skeletal drawings of the donor atoms of both the conformers.

The skeletal diagram of the donor atom shows that the donor atoms of the macrocycle are arranged in a chair conformation. The metal ion is either 8 or 9 coordinated in the major conformer and is either 7 or 8 coordinated in the minor conformer. The higher coordination number arises because the K–07 bond length is 3.26 Å. If this distance is accepted as a bond, then in the major conformer the metal cation is 9 coordinated. The iodide anion is not bonded to the K^+ cation but is hydrogen bonded to the hydrogen on 06. The structural data are seen in Table 9. The metal ion is situated above the plane of the macrocycle. The macrocyclic oxygen donors are closer to the metal ion than the oxygens on the pendent arms, except for 05. The K–N distances are shorter than the K–O distances of the macrocyclic pendent arms. The R value is 1.39 (7–coord), 1.44 (8–coord) and 1.49 (9–coord) and compare well with Shannon's effective ionic radii for the K^+ cation (98).

3.4.2 The structure of [K(BHEE–18–ane N_2O_4)]I

During refinement of the structure of [K(BHEE–18–ane N_2O_4)]I it became apparent that there was disorder in the terminal portion of one of the side arms, represented by the atoms C15–C16–O6. Refinement of the positions and site occupancy factors (SOF) for this disordered fragment indicated the two alternative orientations for C15–C16–O6 [SOF = 0.75(1)] and C15'–C16'–O6' [SOF = 0.25(1)], shown in Fig. 2.5.3c,d. The two disordered individuals differ only in that in the major form the terminal 06 is coordinated to the metal ion, whereas in the minor form it is not. The hydrogen of 06 is hydrogen bonded to an iodide in the same unit cell, whereas that of 06' is hydrogen bonded to an iodide in a neighbouring unit cell. The structure and numbering scheme of the two disordered individuals are shown in Fig. 2.5.3c,d. In Fig. 3.4.2 is seen a stereo view of the major conformer and in Fig. 3.4.3 are seen the skeletal drawings of the donor atoms of both the conformers.

The skeletal diagram of the donor atom shows that the donor atoms of the macrocycle are arranged in a chair conformation. The metal ion is either 8 or 9 coordinated in the major conformer and is either 7 or 8 coordinated in the minor conformer. The higher coordination number arises because the K–07 bond length is 3.26 Å. If this distance is accepted as a bond, then in the major conformer the metal cation is 9 coordinated. The iodide anion is not bonded to the K^+ cation but is hydrogen bonded to the hydrogen on 06. The structural data are seen in Table 9. The metal ion is situated above the plane of the macrocycle. The macrocyclic oxygen donors are closer to the metal ion than the oxygens on the pendent arms, except for 05. The K–N distances are shorter than the K–O distances of the macrocyclic pendent arms. The R value is 1.39 (7–coord), 1.44 (8–coord) and 1.49 (9–coord) and compare well with Shannon's effective ionic radii for the K^+ cation (98).

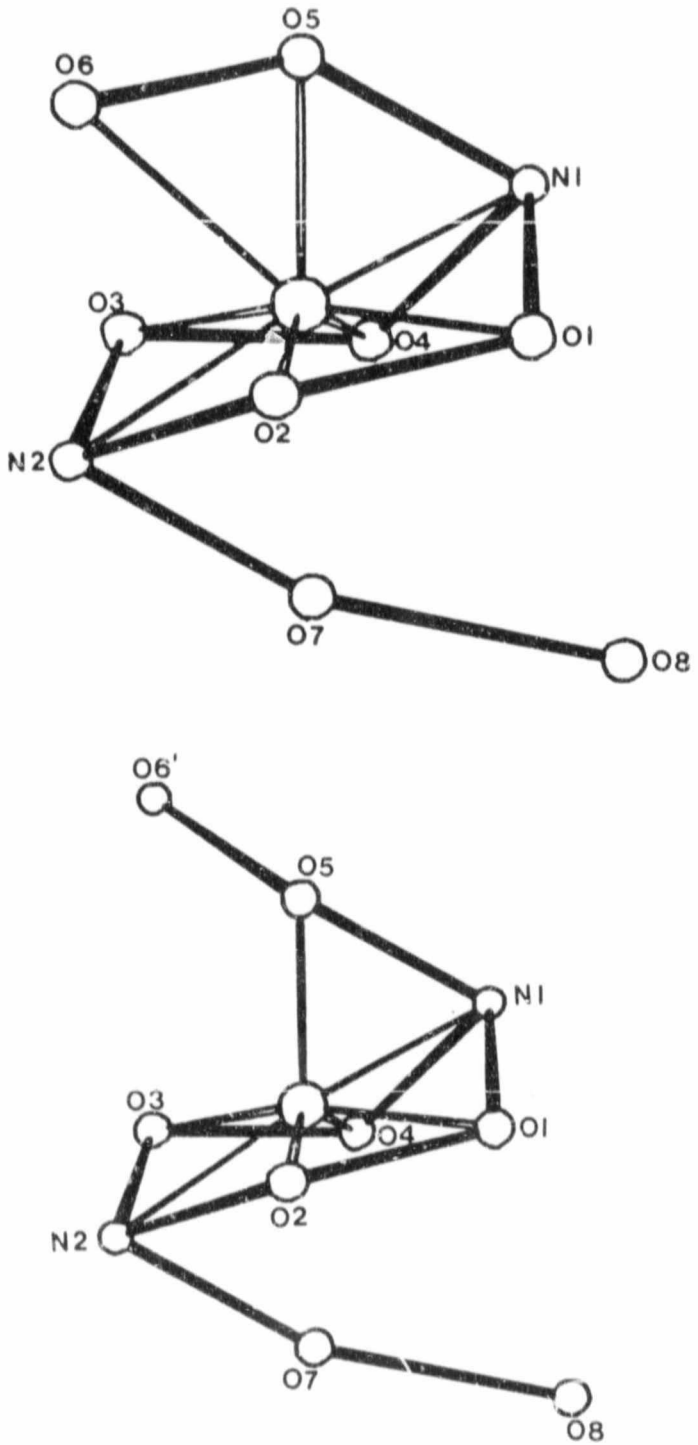

Fig. 3.4.3 Skeletal diagram illustrating the donor atoms of the major conformer (top) and the minor conformer (bottom) of [K(BHEE–18–ane N_2O_4)]I.

There are two ways in which metal complexation can occur in macrocycles containing two pendent arms. Binding can take place from the same side of the macrocycle (cis–arrangement) or from opposite sides of the macrocycle (trans–arrangement). Gokel et al. (113) refer to these as the syn– and anti–arrangements. In the sterically less crowded $[K(BHE–18–ane\ N_2O_4)]^+$ complex the pendent arms occupy the cis–orientation with all donor atoms coordinated. Since the pendent arm oxygens are alcoholic oxygens and more polar, these donor atoms can get closer to the metal ion when the macrocycle adopts the boat conformation. Therefore, shorter K–O bond lengths are observed for the pendent arms. In the sterically more crowded $[K(BHEE–18–ane\ N_2O_4)]^+$ complex the pendent arms occupy the trans–orientations with at least two of the oxygen donors on the pendent groups being left uncoordinated. Thus, the high level of steric crowding exhibited in the $[K(BHEE–18–ane\ N_2O_4)]^+$ structure is evident since even a large metal ion such as the K^+ cation cannot coordinate to all the donor atoms. The interaction of the pendent arm donor atoms in the sterically more crowded ligand is less than in the $[K(BHE–18–ane\ N_2O_4)]^+$ complex as indicated by the respective bond lengths.

The above results are consistent with those reported by Gokel et al. (113) for similar K^+ complexes of N,N–disubstituted 18–aneN_2O_4 derivatives. The authors found that with sterically less crowded ligands of this type, the pendent arms occupy the cis–orientations whereas pendent arms in the sterically more crowded ligands occupied the trans–orientation, with the macrocycle in the boat and chair conformation respectively. Thus, the trans–arrangement of the pendent groups may be a response to steric crowding.

3.4.3 The Structure of $[Ba(BHEE–18–ane\ N_2O_4)]I_2$

The structure and numbering scheme of the complex is given in Fig. 2.5.3b. The unit cell packing diagram is seen in Fig. 3.4.4 and the skeletal diagram of the donor

atoms is seen in Fig. 3.4.5. The skeletal diagram shows the donor atoms of the macrocycle to be arranged in a boat conformation. The metal ion is eleven coordinate since the oxygen of the water is also coordinated. The complex lies on a two fold axis. The oxygen donor of the water molecule occupies a true apical position below the macrocycle. The pendent arm alcoholic oxygen donors occupy positions above the macrocycle, slightly skewed from true apical. The alcoholic oxygen donors are closer to the metal ion than the ethereal oxygen donors of the pendent arms. The K–N distances are longer than the K–O bond lengths. The N–M–N angle is 170°. The R value is 1.50Å and compares well with Shannon's effective ionic radii (98).

All the donor atoms of BHEE–18–ane N_2O_4 are effectively involved in coordination to the Ba^{2+} metal ion. This is surprising since for the similarly sized K^+ cation at least two oxygen donors were uncoordinated. The participation of the extra oxygen donors in coordination thus accounts for the increase in complex stability observed for the Ba^{2+} complex with BHEE–18–ane N_2O_4 compared to the presumably eight–coordinate complex of Ba^{2+} with DHP–18–ane N_2O_4.

In order to investigate why two similarly sized metal ions should show different conformations when complexed to the same ligand it was necessary to perform molecular mechanics calculations on the K^+ and Ba^{2+} complexes of BHEE–18–ane N_2O_4. The initial structures used were those from crystal structures. The total strain energies obtained for the two complexes are given in Table 10. The K^+ 8–coordinate conformer (-16.7 kcal.mol^{-1}) was generated from the Ba^{2+} structure, and energy minimized, whereas the conformer with the higher energy (-10.6 kcal.mol^{-1}) was generated from the Ba^{2+} structure with modified O–donor coordinates and refined. The 9–coordinate conformer was generated from the K^+ structure and the 10–coordinate conformer was generated from the Ba^{2+} structure. The Ba^{2+} 9–coordinate conformer was generated from the K^+ structure

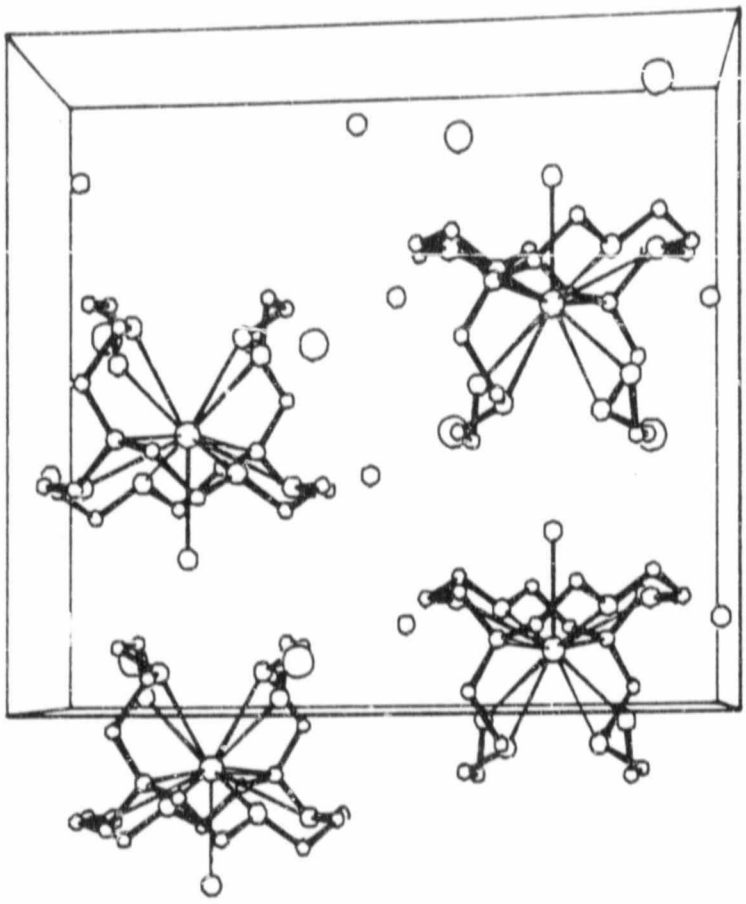

Fig. 3.4.4 The unit cell packing diagram of $[Ba(BHEE-18-ane\ N_2O_4)]I_2 \cdot 3H_2O$

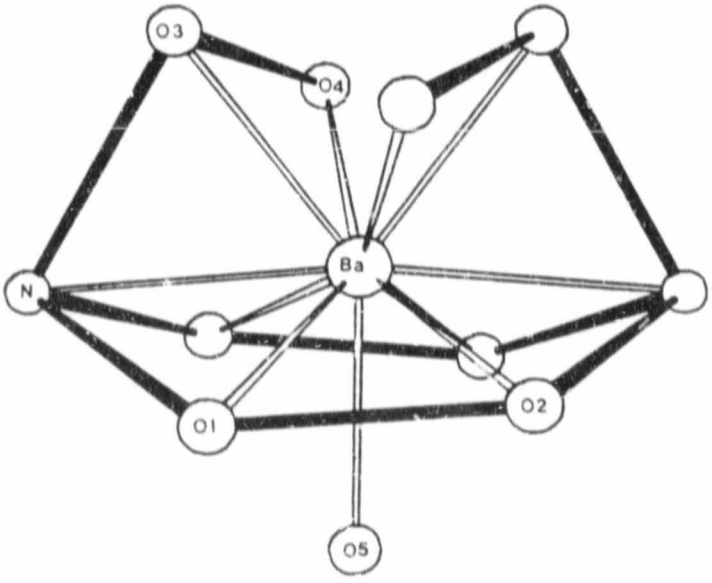

Fig. 3.4.5 Skeletal diagram illustrating the donor atoms of $[Ba(BHEE-18-ane\ N_2O_4)]I_2 \cdot 3H_2O$

and the Ba^{2+} 10–coordinate conformer was generated from the Ba^{2+} structure without the water molecule. The water molecule was removed from the $[Ba(BHEE–18–ane\ N_2O_4)]^{2+}$ so that comparison could be made with the strain energy obtained for the $[K(BHEE–18–ane\ N_2O_4)]^{+}$ complex. From the data given in Table 10 it can be seen that the lowest strain energy for K^+ complex occurs when K^+ is nine coordinate, whereas for the Ba^{2+} complex minimum strain energy is observed when the cation is ten–coordinate. That is, minimum strain energies are obtained for the structures observed in the crystal structures of the two metal cation complexes.

Inspection of the data given in Table 11 shows that when Ba^{2+} adopts a lower coordination number its effective ionic radius decreases. Thus, 9–coordinate K^+ and Ba^{2+} metal ions have effective ionic radii of 1.55 and 1.47Å respectively. In other words, Ba^{2+} is effectively "smaller" than the K^+ metal ions when it is 9–coordinate. Smaller metal ions are more sensitive to increase in steric strain and to overcome this strain, Ba^{2+} adopts a coordination of eleven, where its effective ionic radius is larger, of about 1.56Å. The question that comes to mind then is why the K^+ ion prefers to be 9–coordinate instead of 10–coordinate where its effective ionic radius is in fact larger than if it were 9–coordinate. One would suggest that there is a contribution from the cavity size of the macrocycle. It is seen that 9–coordinate K^+ and 11–coordinate Ba^{2+} have about the same effective ionic radii, which is probably the "best–fit" metal ion size. With 10–coordinate K^+ the effective radius becomes 1.59Å, a little too large for the cavity, which would result in an increase in strain energy, as observed in Table 10. Thus, to be best accommodated by the macrocyclic cavity K^+ adopts 9–coordination and does so best with the pendent arms in the trans–orientation whereas Ba^{2+} prefers to be 11–coordinate with the pendent arms in the cis–orientation.

Table 10 Total strain energies, Σ U, for the K^+ and Ba^{2+} complexes of BHEE–18–ane–N_2O_4

Coordination No	Total Strain Energy ΣU (kcal·mol^{-1}) 8	9	10
K^+	−16.7[a] −10.6[b]	−18.7	−10.5
Ba^{2+}		−350.9	−354.2

a,b different conformations observed.

a both alcoholic oxygens non–coordinating.

b oxygen donors of one pendent arm coordinates whereas those of the second pendent arm do not participate in coordination.

Table 11 Effective Ionic Radii (Å) of the Potassium and Barium cations as a function of the Number of Donors

Coordination No	Effective Ionic Radii (Å) K^+	Ba^{2+}
6	1.38	1.36
8	1.51	1.42
9	1.55	1.47
10	1.59	1.52
12	1.60	1.60

Data from Ref. 98

Another important factor contributing to the type of conformation adopted by the ligand is the charge on the metal ion. The K^+ metal ion is univalent and has a smaller positive charge than the divalent Ba^{2+} cation. The different charges of the metal ions would suggest that in the case of Ba^{2+}, the greater positive charge is able to overcome the unfavourable electrostatic repulsions between the negatively charged oxygen donors and so pull the pendent arms inwards to give the cis–arrangement. With the K^+ ion, because of its lower charge it is unable to overcome the electrostatic repulsion between the oxygen–donors on the arms and thus the pendent arms are arranged in the trans–arrangement.

All of the correlations examined in this study have involved divalent metal ions, so that the effect of charge on the cation on the effect of added O–donors remains unclear. However, for the effect of five– versus six–membered chelate rings on metal ion size–based selectivity, it is seen in Fig. 3.4.6 that metal ions of differing charges show different correlations of Δ log K versus r^+. In Fig. 3.4.6 the change in complex stability for a variety of metal ions is plotted against ionic radius. The pair of ligands where the change is occurring are EDTA and TMDTA. The ligand EDTA forms a five–membered chelate ring whereas TMDTA forms a six–membered chelate ring on complex formation. In previous discussions it has been emphasized that five–membered chelate rings favour the complexation of large metal ions whereas six–membered chelate rings favour the complexation of small metal ions. The discussions were, however, limited to divalent metal ions. Although the response of the metal ion to change in chelate ring size is largely dependent on the size of the metal ion, Fig. 3.4.6 strongly suggests that there is a definite contribution from the charge of the metal ion. Thus, as the charge on the metal ion increases, so the slope of the correlation becomes steeper, showing that with increasing charge metal ions become more sensitive to the size of the chelate ring. This would seem to relate to increasing covalence in metal ions of the same size but higher charge, which requires a stronger directionality in the M–N bond.

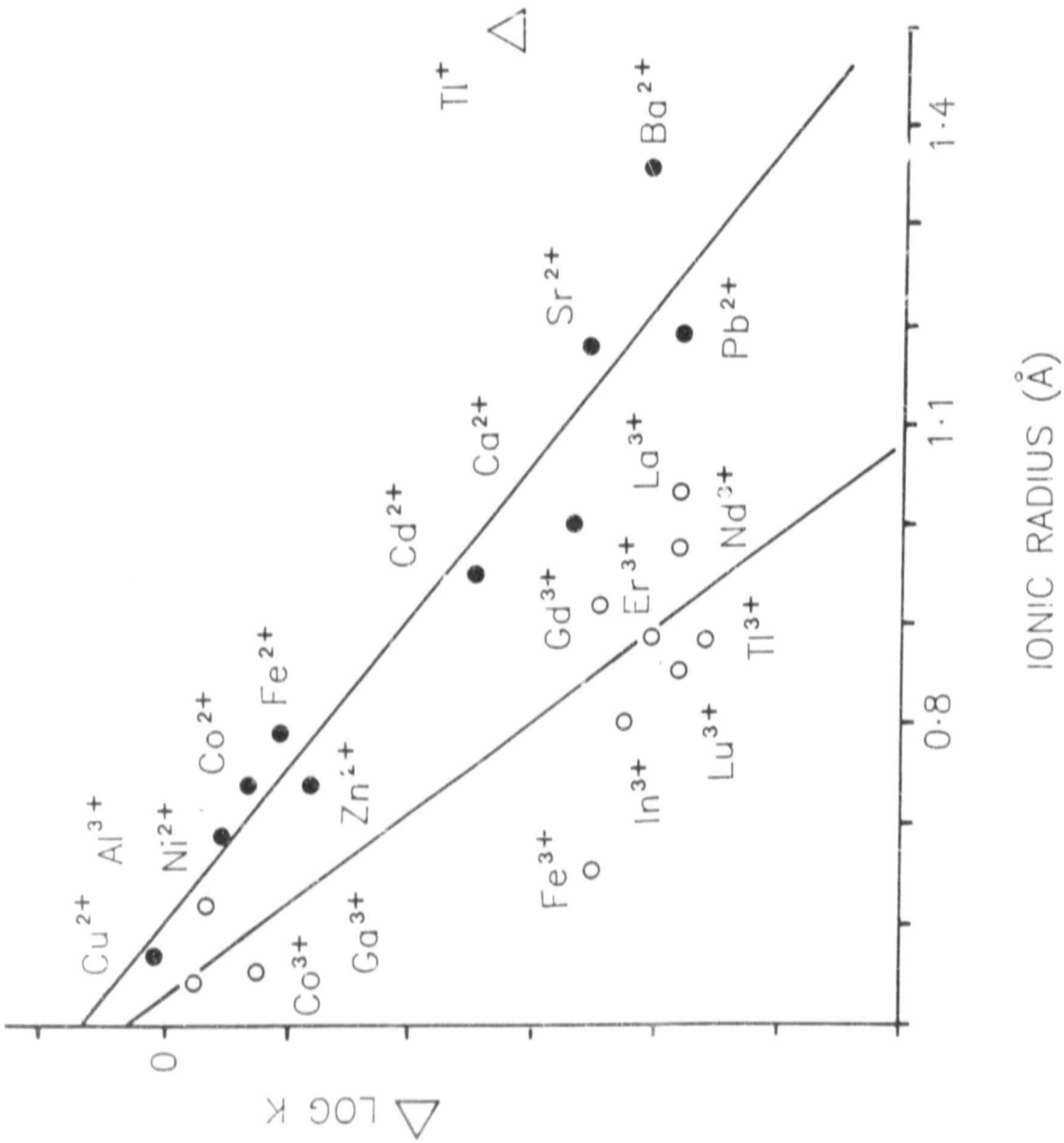

Fig. 3.4.6 Relationship between change in complex stability, Δ log K, which occurs when changing a five–membered chelate ring to a six–membered chelate ring, and the ionic radius (98) of the metal ion.

3.5 THE COMPLEX STABILITY OF ALKALI CATIONS WITH MACROCYCLES CONTAINING OXYGEN DONORS

Since the pioneering work of Pedersen (2), the interest in crown ethers and cryptands has increased considerably. The complexes of these compounds have received much attention, not only because of their importance in coordination chemistry, but also because these complexes exhibit potential significance in biological systems particularly with respect to ion transport and antibiotics. The association of alkali cations with crown ethers have been mainly described in terms of "hole–size–selectivity", that is, maximum complex stability occurs when the size of the metal ion matches the cavity in the center of the macrocycle (2,48). More recent evidence (27,28,57,59) suggests that the key factor in controlling cation selectivity in macrocycles containing oxygen donors is the number of oxygen donors present rather than the macrocyclic cavity. The size selectivity demonstrated by these macrocyclic ligands has been explained in terms of the balance between steric and inductive effects (100). Thus, for 18–crown–6 the stability of metal complexes is $Li^+ < Na^+ < K^+ > Rb^+ > Cs^+$. This stability order does not reflect the better fit of K^+ cation into the cavity of 18–crown–6, but rather reflects the order of the M–O bond strength (100). The demonstration of cation selectivity by these oxygen donor macrocycles has resulted in the use of these compounds in many areas where this property is important (3,116), for example, in cation selective electrodes, study of biological transport mechanism etc. Much research has therefore been focussed on the determination of the complex stability of the alkali metal ions with oxygen donor containing macrocycles.

Frensdorff (48) has reported the stability of a large number of crown ether complexes with alkali cations and Lehn et al. (63,112) have studied the complexes of alkali metal cryptates extensively. More recently Gokel et al. (113) have reported stability constants for a series of "lariat ethers" with alkali metal ions.

The results (113) indicate that alkali binding by "lariat ethers" is enhanced by the presence of sidearm donor groups. As an extension to the study of the relative contribution of pendent donor groups to the binding strength of alkali metal ions, the complexation properties of a series of ligands with a few alkali metal ions is reported.

The stability constants of the alkali metal ions with the macrocycles shown below have been determined using NMR of the alkali nuclei. The chemical shifts were determined as a function of ligand/M^+ mole ratio. The data are given Appendix 1.

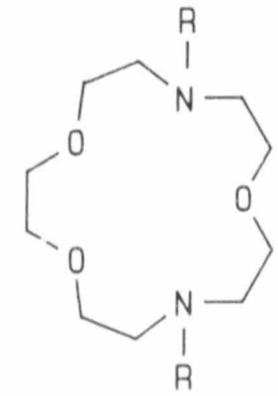

R=H (15-aneN_2O_3)

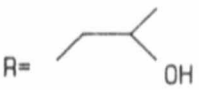

(DHP-15-aneN_2O_3)

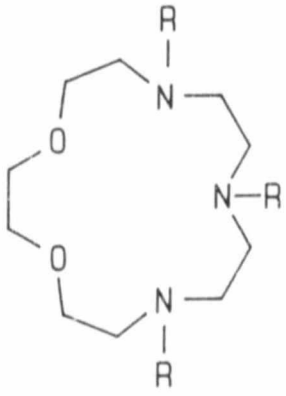

R=H (15-aneN_3O_2)

(THP-15-aneN_3O_2)

In all the spectra recorded only one population average resonance of the metal observed, indicating that cation exchange is fast at 23°C. In Fig. 3.5.1, the relationship between ligand/metal ion mole ratio versus chemical shift is seen. With the unsubstituted macrocycles, a total shift of only 0.2 – 2 Hz from the uncomplexed metal position had been induced. This value, while experimentally

;nificant, indicates an exceedingly weak interaction. The ^{23}Na and ^{87}Rb resonance were considerably broader than that of ^{133}Cs. In all the unsubstituted macrocycle–metal ion complexes there was no additional line broadening accompanying the increase in L/M^+ ratio (Fig. 3.5.2 – 3.5.7). The metal resonance appears to be almost independent of the ligand to metal mole ratio. This type of behaviour indicates that the environment of the metal ion is not changed significantly upon addition of ligand and a weak complex is formed.

With the macrocycles containing pendent donor groups, the metal resonance is dependent on the ligand to metal mole ratio. No levelling off in chemical shift is observed (Fig. 3.5.1). This seem to indicate the formation of a weak 1:1 complex between the metal ion and the ligand. This type of behaviour has been observed by Shamsipur and Popov (115). Their work on 18–ane N_2O_4 indicated that while Li^+, Na^+ and Tl^+ formed 1:1 complexes with 18–ane N_2O_4 (chemical shifts begin to level off at a mole ratio of 1:1), the Cs^+ ion formed a weak 1:1 complex with 18–ane N_2O_4 (chemical shift did not reach a limiting value) in solvents such as nitrobenzene, acetonitrile and acetone. With the ligand–Na^+ and ligand–Rb^+ complexes, the gradual increase in ligand/metal ion mole ratios resulted in a very large increase in the linewidth of the complexed metal ion. The signal was completely eliminated at a mole ratio of approximately 1. This is shown in Fig. 3.5.2b and 3.5.3b. This type of line broadening has been reported by other workers. Popov et al. (117) observed that addition of an equimolar amount of dicyclohexyl–18–crown–6 to a Na^+ solution in nitromethane completely eliminated the ^{23}Na signal. A similar increase in linewidth was reported by Grotens et al. (118) for the benzosubstituted 18–crown–6–Na^+ complex. The ^{87}Rb NMR measurements involving crown or cryptate complexes were reported by Dye et al. (119). The linewidth of cryptand–2,2,2–Rb^+ resonance was too broad to be measured. The linewidth of the ^{133}Cs is very narrow and was found to be in the order of 0.6 – 1.1 Hz. Broadening of linewidths did not accompany the increase in

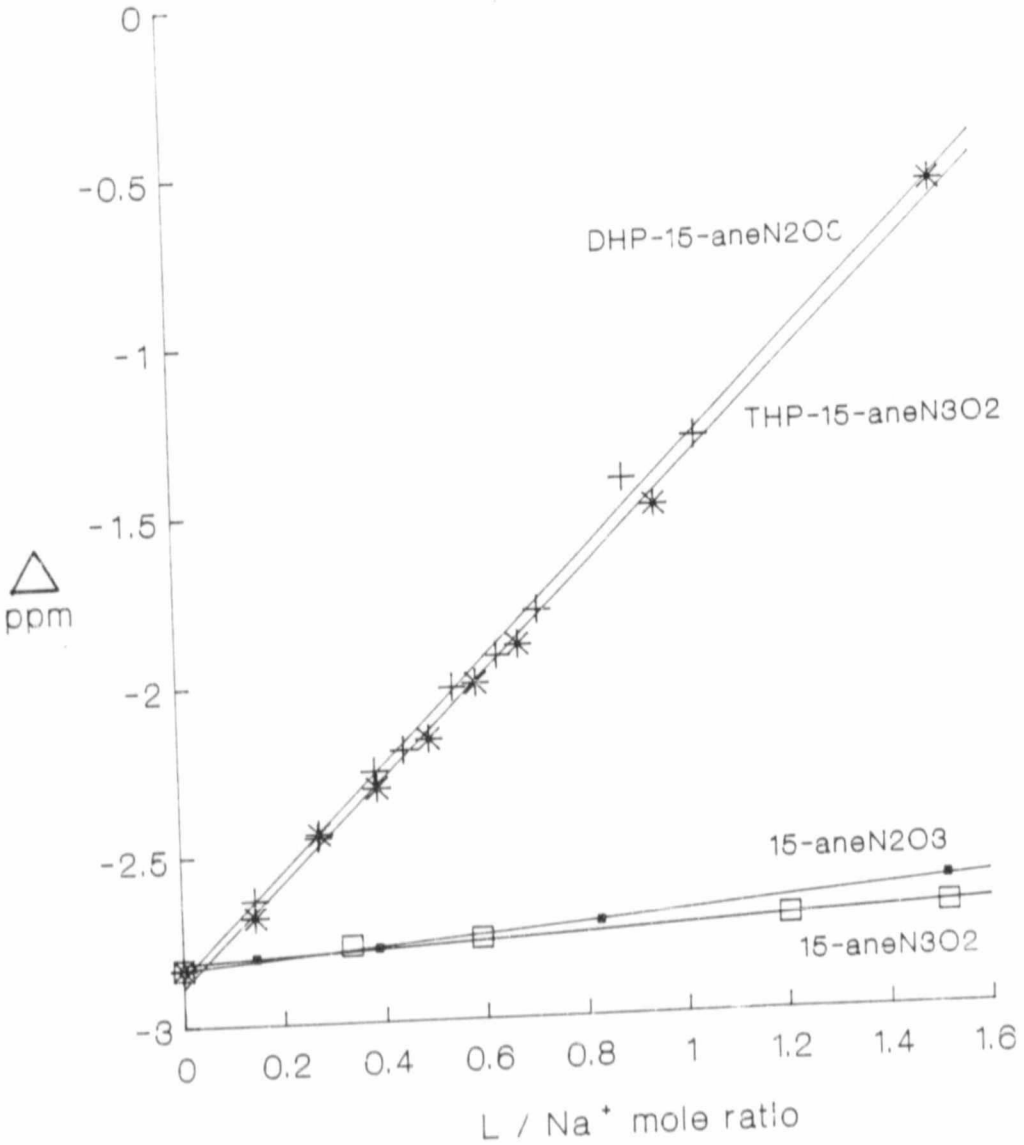

Fig. 3.5.1a ^{23}Na chemical shifts as a function of ligand/M^+ mole ratio in methanol.

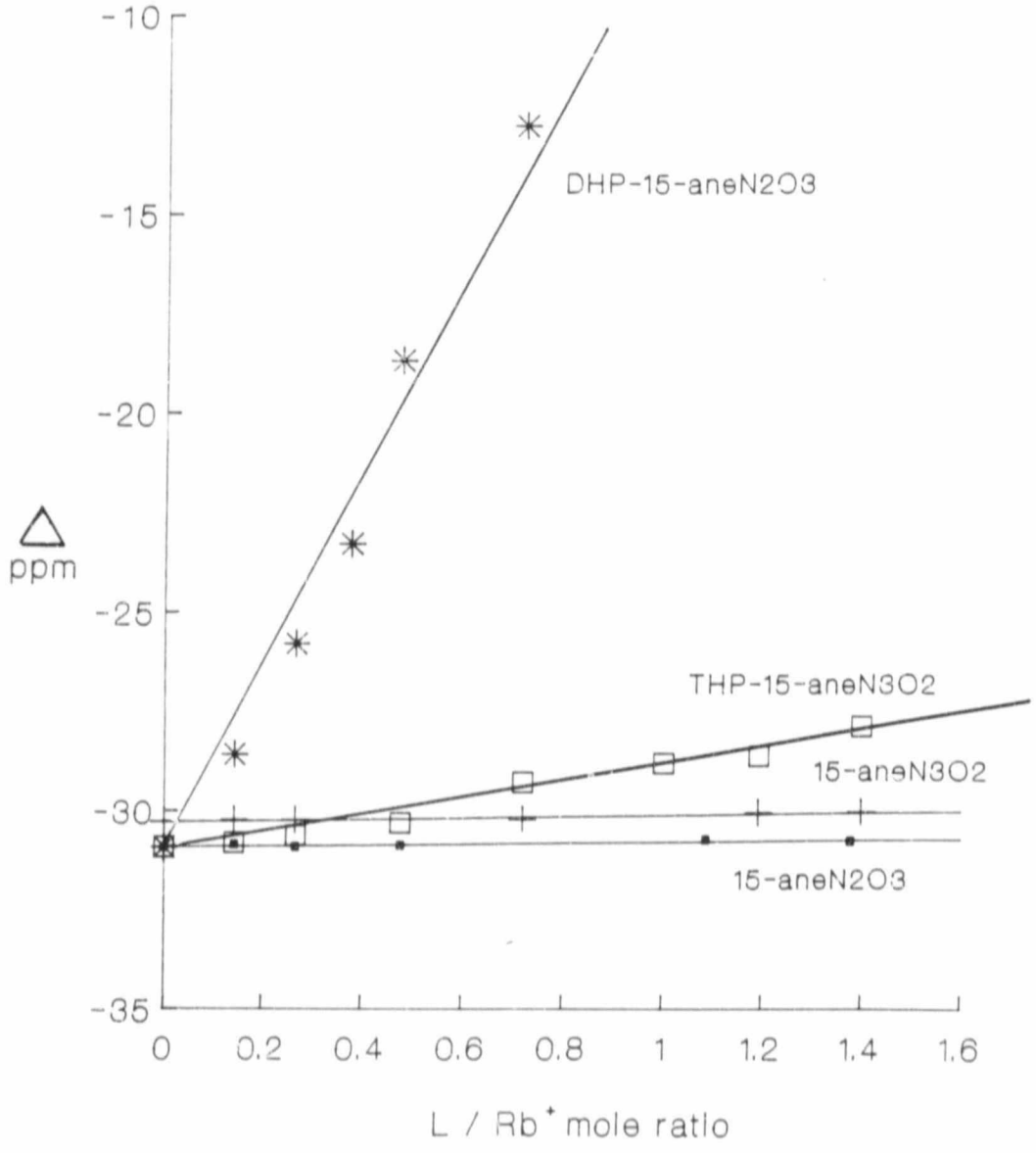

Fig. 3.5.1b ^{87}Rb chemical shifts as a function of ligand/M^+ mole ratio in methanol.

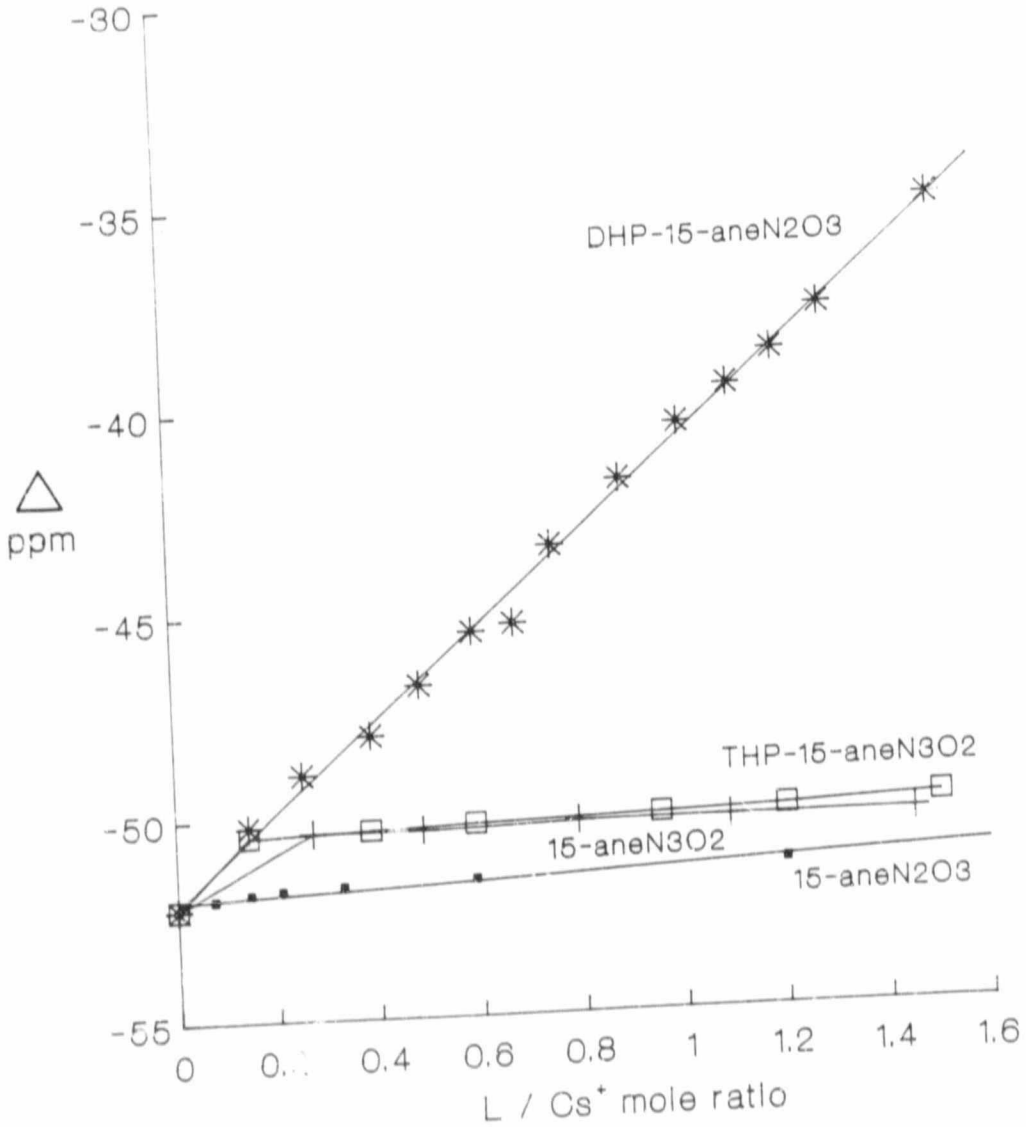

Fig. 3.5.1c ^{133}Cs chemical shifts as a function of ligand/M^+ mole ratio in methanol.

ligand/M^+ mole ratios. The resonance shifted linearly with increase in ligand to metal ion mole ratio and no levelling off in chemical shift occurred, indicating a weak 1:1 complex formation. There is no evidence of the formation of a 1:2 (metal to ligand) complex, such as that reported by Mei et al. (120,121) for the 18–crown–6–Cs^+ complex. Mei et al. (120,121) found that in the ^{133}Cs-NMR studies of 18–crown–6–Cs^+ in pyridine solutions the resonance shifted downfield until a L/M^+ mole ratio of 1:1. Upon further addition of ligand, that is, at higher L/M^+ mole ratios, the resonance shifted upfield. This type of behaviour indicated two different complexes, the formation of a 1:1 crown complex followed by the addition of a second molecule of the ligand to give a 2:1 complex (120,121). Similar behaviour was observed by Live and Chan (122) in the proton NMR of 18–crown–6–Cs^+.

The formation constants were calculated by the method given in Section 2.4.2. The results are shown in Table 12. It must be noted that the values of the Na^+ and Rb^+ complexes with the substituted macrocycles are not very accurate since line broadening at high L/M^+ mole ratio made the determination of the chemical shift difficult. The formation constant was found to be sensitive to the value of n_∞, that is, chemical shift of metal when infinite amount of ligand is added.

Table 12. Formation constants (log K_1) of some alkali metal ion complexes with various ligands studied in methanol at 23°C

Ligand	Li^+	Na^+	K^+	Rb^+	Cs^+
15–ane N_2O_3	–	<1	–	<1	<1
DHP–15–ane N_2O_3	–	2.9(3)	–	2.0(3)	1.80(8)
15–ane N_3O_2	–	<1	–	<1	<1
THP–15–ane N_3O_2	–	1.8(2)	–	1.3(3)	1.4(7)

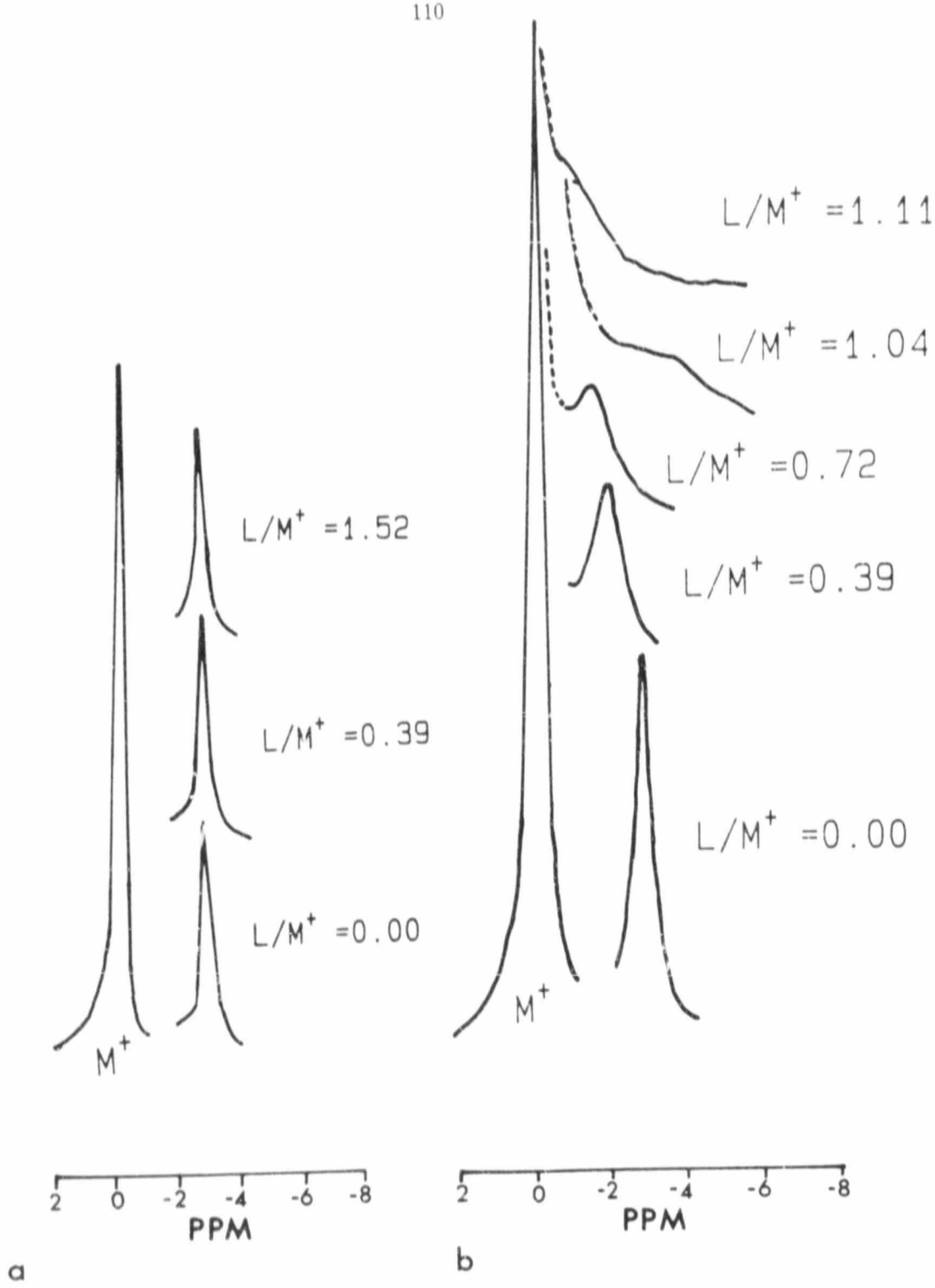

Fig. 3.5.2 ^{23}Na NMR spectra of a) Na^+–15–ane N_2O_3 and b) Na^+–DHP–15–ane N_2O_3 in methanol at 23°C.

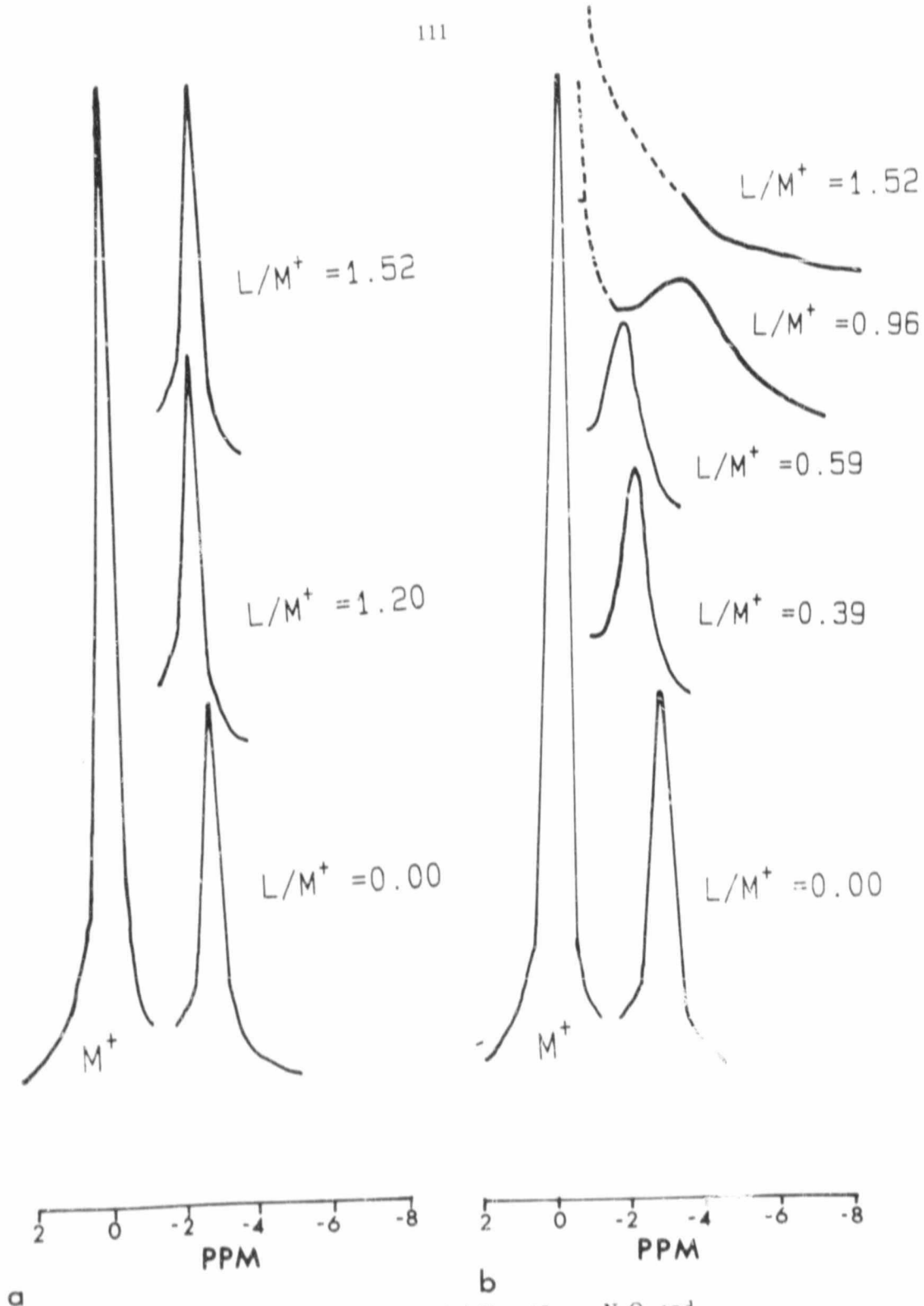

Fig. 3.5.3 ^{23}Na NMR spectra of a) Na^+–15–ane N_3O_2 and b) Na^+–THP–15–ane N_3O_2 in methanol at 23°C.

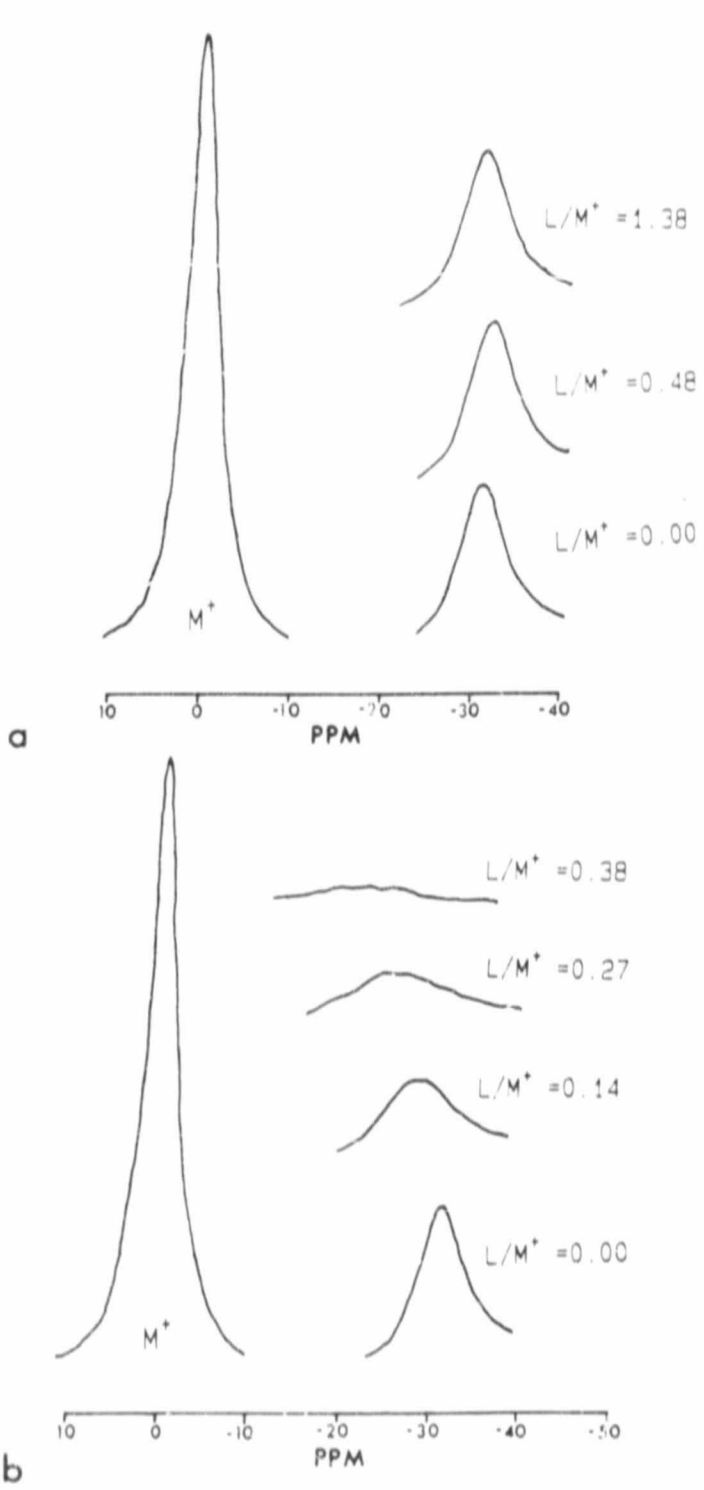

Fig. 3.5.4 ^{87}Rb NMR spectra of a) Rb^+–15–ane N_2O_3 and b) Rb^+–DHP–15–ane N_2O_3 in methanol at 23°C.

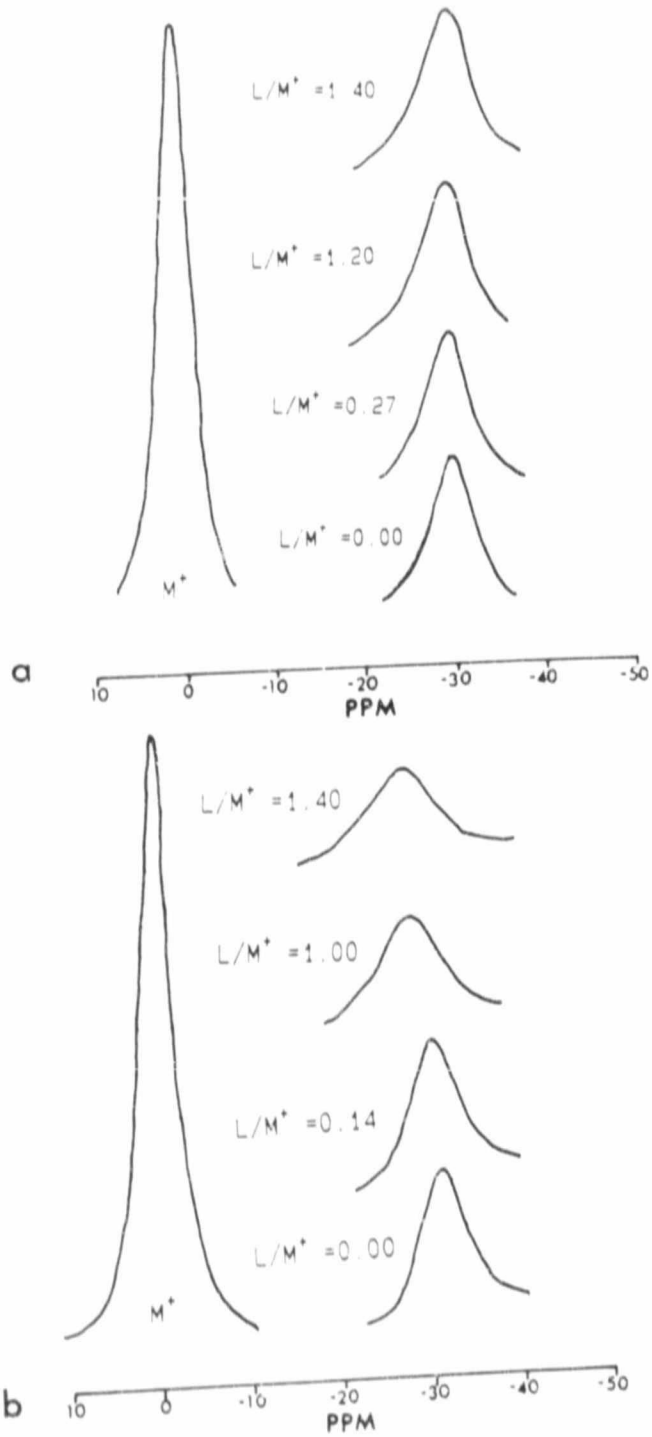

Fig. 3.5.5 ^{87}Rb NMR spectra of a) Rb^+–15–ane N_3O_2 and b) Rb^+–THP–15–ane N_3O_2 in methanol at 23°C.

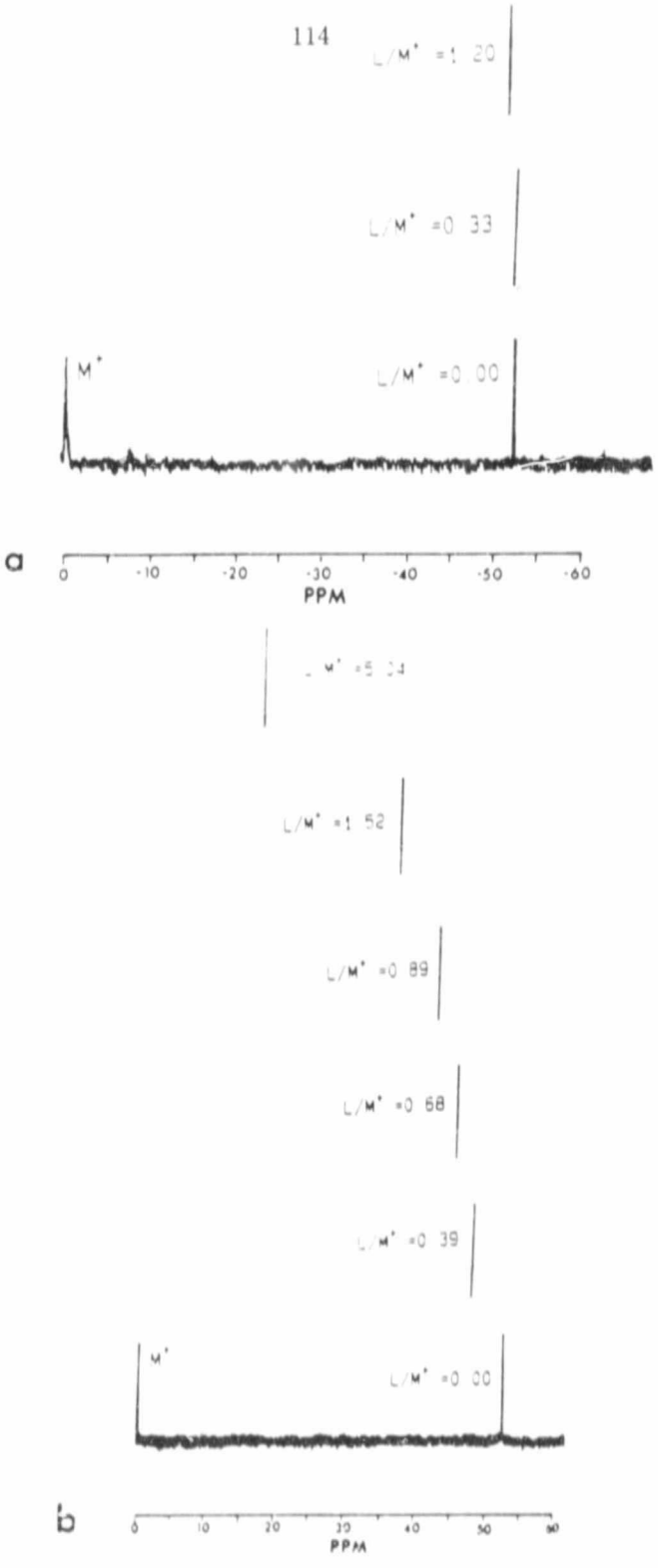

Fig. 3.5.6 ^{133}Cs NMR spectra of a) Cs^+–15–ane N_2O_3 and b) Cs^+–DHP–15–ane N_2O_3 in methanol at 23°C.

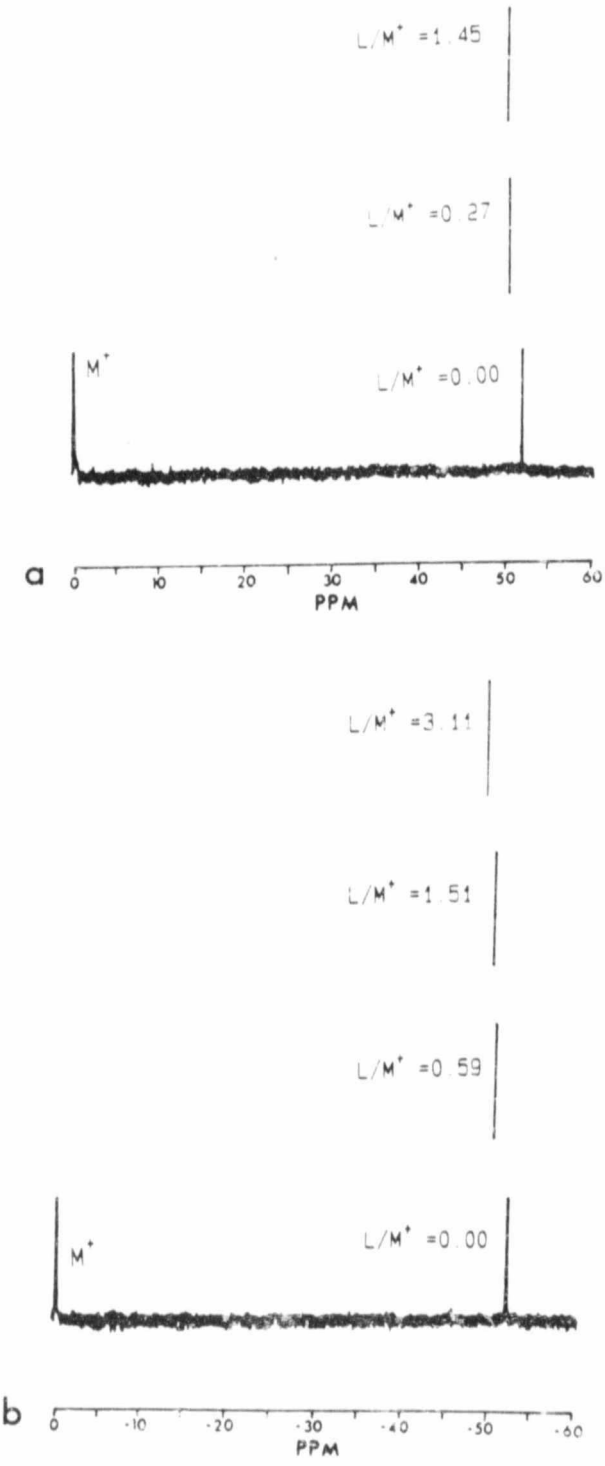

Fig. 3.5.7 ^{133}Cs NMR spectra of a) Cs^+–15–ane N_3O_2 and b) Cs^+–THP–15–ane N_3O_2 in methanol at 23°C.

The formation constants of all the unsubstituted macrocycles with the metal ions studied were found to be less than 1 log unit. The extremely weak interaction between the macrocycle and cation is reflected in the respective chemical shifts observed in the NMR spectra (Fig. 3.5.2 – 3.5.7). The weak complexation was as expected. Frensdorff (48) reported the effect of nitrogen and sulfur substitution on the stability constants of 18–crown–6 derivatives. The stability constants were determined in methanol and it was found that substitution of N or S for O in 18–crown–6 and dibenzo–18–crown–6 greatly weakened the stability of K^+ complexes. Similar behaviour is observed for the 15–crown–5 complexes. As seen in Fig. 3.5.8, replacement of a single O–donor by an N–donor causes a sharp decrease in complex stability of approximately 2.5 log units.

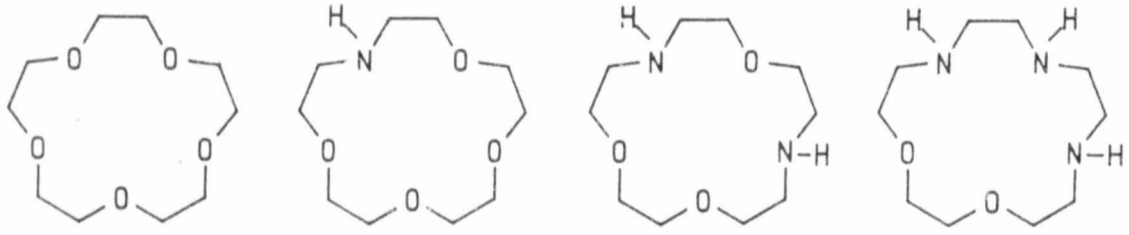

Fig. 3.5.8 Effect of N–substitution on complex stability of alkali cation complexes. [a] Ref. 114

The substitution of a second oxygen donor will therefore lead to a larger decrease in complex stability and it is not surprising to find that only very weak complexes are formed (<1 log unit) when two or more oxygens are replaced by nitrogen donors. The decrease in complex stability is due to the decrease in electronegativity of the substituted nitrogen donor. As the negative charge on the donor atom drops,

the electrostatic forces between the donor and the cation decrease, resulting in a decrease in complex stability.

An enhancement in complex stability is observed for all the complexes formed when extra oxygen donors are added to the macrocycle in the form of pendent arms. Thus, addition of oxygen donors increases the binding strength of alkali metal ions. Irrespective of the macrocycle containing pendent arms, maximum stability was observed with the complexes formed with the Na^+ cation. Both the macrocycles studied are 15–membered rings, differing only in the number of nitrogen donors. Thus, the ring which has the larger number of nitrogen donors form complexes which have poorer binding strengths. For the Na^+ complex there is a decrease of ~1 order of magnitude in the log K values in going from DHP–15–ane N_2O_3 to THP–15–ane N_3O_2, for the Rb^+ complex a decrease of 0.7 log units and for the Cs^+ complex a decrease of 0.4 log units. These results are not as expected since Cs^+ ion is a "harder" acid than Na^+ and should interact less strongly with the nitrogen donors of the ring. A sharper decrease was thus expected for the THP–15–ane N_3O_2 – Cs^+ complex relative to the DHP–15–ane N_2O_3 – Cs^+ complex.

The above results strongly emphasize that addition of oxygen donors increases the complex stability of the alkali metal ions. However, as discussed in previous sections, the addition of oxygen donors to existing ligands produces metal ion size–selectivity where larger metals show an increase in complex stability relative to the smaller metal ions. This type of behaviour cannot be deduced from the above results since the magnitude of the log K_1 values of the unsubstituted macrocycles are not exactly known. However, addition of oxygen donors to the macrocycle has increased the complex stability of all the metal ions and the order of stability is $Na^+ > Rb > Cs^+$. These results are not consistent with those reported by Gokel et al. (114). In Fig. 3.5.9 is seen the effect on complex stability upon

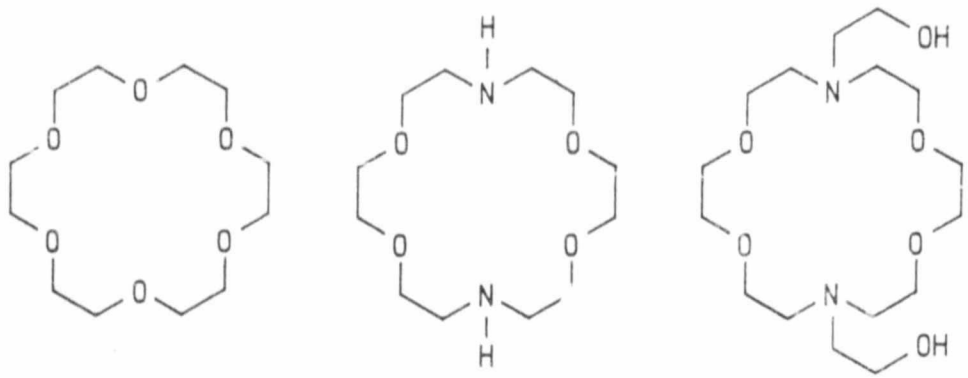

18-crown-6	18-aneN_2O_4	BHE-18-aneN_2O_4
$LogK_1(Na^+)$ [a]: 4.35	2.04	4.87
$LogK_1(K^+)$ [a] : 6.08	1.8	5.08

Fig. 3.5.9 Effect of addition of oxygen donors on the complex stability of alkali metal ions. [a] Ref. 114 (log K values determined in methanol).

addition of oxygen donors. The stability order of the complexes formed with 18–ane N_2O_4 is $Na^+>K^+$. Upon addition of alcoholic oxygen donors to the macrocycle the order becomes $K^+>Na^+$. Thus, addition of oxygen donors increases the selectivity of larger over small metal ions. It must be noted that the above macrocycles form 18–membered rings whereas those reported in this work form 15–membered rings. The stability order $Na^+>Rb^+>Cs^+$ in the latter macrocycles suggests that while cavity size may not play an important role in controlling size–selectivity, there is a definite contribution from it. Thus, for the smaller macrocycle DHP–15–ane N_2O_3 the order in complex stability is $Na^+>Rb^+>Cs^+$ and $Ca^{2+}>Sr^{2+}>Ba^{2+}$ (section 3.1) whereas for the larger macrocycle DHP–18–ane N_2O_4 the stability order for the alkaline earth metal ion was $Ba^{2+}>Sr^{2+}>Ca^{2+}$ (Section 3.1). It would be of interest to study the complexation properties of the latter ligand with the alkali metal ions. The predicted order of complex stability would be $K^+>Na^+>Li^+$, on the basis of cavity size and metal ion size. Gokel et al. (114) has shown that K^+ cation binding is enhanced in the presence of pendent

arms bearing oxygen donors. As can be seen in Fig. 3.5.9, the increase in complex stability in going from 18–ane N_2O_4 to BHE–18–ane N_2O_4 for the K^+ complex is 3.28 log units. This arises because of the participation of the extra oxygen donors in binding (114). The binding can be enhanced even further by the addition of extra oxygen donors either in the form of pendent arms or in the macrocycle itself. The ligand BHEE–18–ane N_2O_4 will thus prove to be of interest.

Much of the observed selectivities of the crown ethers and open–chain ethers with alkali cations has been related to the coordinating properties of the neutral oxygen donor (28,29,57). In Fig. 3.5.10 are shown the formation constants of a variety of ligands with the alkali metal ions, as a function of crystal radius. The order of complex stability is $Li^+<Na^+<K^+>Rb^+>Cs^+$. The order $Li^+<Na^+<K^+$ reflects the degree of steric crowding. Thus, as the metal ion becomes smaller, as in the case of Li^+ and Na^+, steric crowding around the metal ion increases when the ligand coordinates to it, and leads to a decrease in complex stability (100). The peak in complex stability does not reflect a better fit of the K^+ cation into the macrocyclic cavity. In fact, molecular mechanics calculations (31) reveal that with 18–crown–6, the Cs^+ cation coordinates with less strain energy than the K^+ cation. The stability order $K^+>Rb^+>Cs^+$ is in fact a reflection of the order of M–O bond strength $K^+>Rb^+>Cs^+$ (31,100). The final stability order is thus derived from the different components of energies. This is shown in Fig. 3.5.11 for 18–crown–6.

In order to study the effect of the addition of oxygen donors on alkali metal ion specificty, molecular mechanics calculations were carried out on the alkali complexes of 18–ane–N_2O_4, BHE–18–ane–N_2O_4 and BHEE–18–ane N_2O_4. In this series there is a gradual increase in the number of oxygen donors with a progressive increase in steric strain. The program used for the molecular mechanics calculations is a locally modified (by P.W. Wade) version of MOLBLD3 (130) for

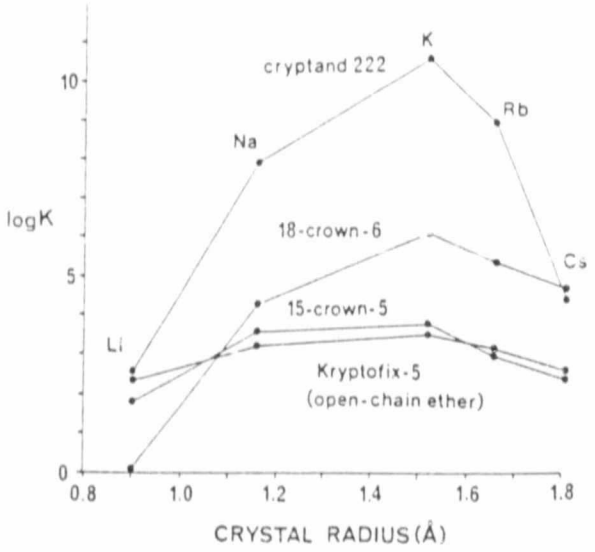

Fig. 3.5.10 Formation constants, log K_1, in methanol for a variety of ligands complexing with the alkali metal ions, as a function of crystal radius. Reproduced with permission from Ref. 100.

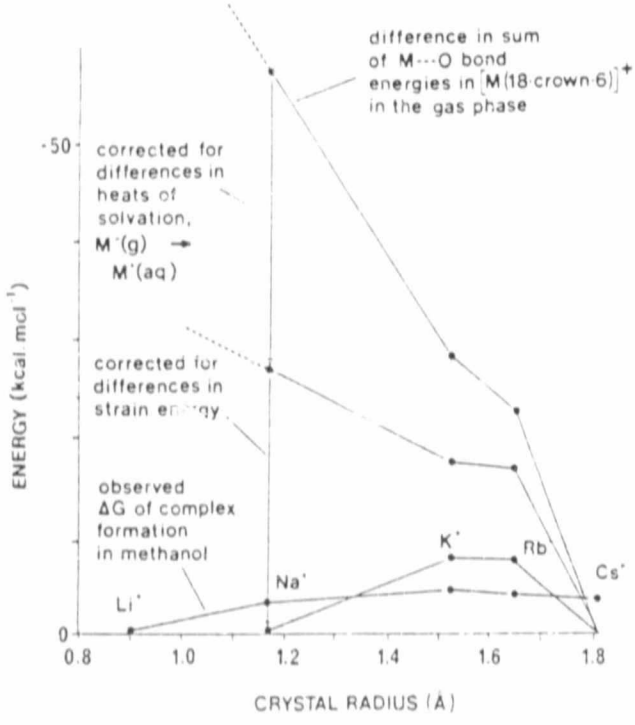

Fig. 3.5.11 The components of the energies contributing to the final stability order observed for 18–crown–6 complexes with the alkali metal ions, as a function of radius. Reproduced with permission from Ref. 100.

the united atom approach (129). The force field parameters used for a) the ligands are due to Kollman et al. (127), b) for Na^+, K^+, Rb^+ and Cs^+ are due to Wipff et al. (31) and c) for Li^+ are due to Kollman et al. (128) The total strain energy obtained for the alkali complexes are listed in Table 13.

Table 13 Total strain energy (ΣU) obtained for the alkali metal ion complexes with a variety of ligands

	Total strain Energy/kcal. mol^{-1}			ΔU (2–1)	ΔU (3–2)
	18–aneN_2O_4(1)	BHE–18–ane N_2O_4(2)	BHEE–18–ane N_2O_4(3)		
Li^+	–138.1	–92.6	–40.8	45.5	51.8
Na^+	–115.4	–80.7	–29.7	34.7	51.0
K^+	–95.3	–65.8	–18.7	29.7	47.1
Rb^+	–87.6	–59.2	–10.7	28.4	48.5
Cs^+	–73.3	–50.8	+5.3	22.5	45.5

In Fig. 3.5.12 is seen the change in strain energy in going from 18–aneN_2O_4 to BHE–18–aneN_2O_4 and BHE–18–aneN_2O_4 going to BHEE–18–aneN_2O_4. The figure thus represents the change in strain energy upon addition of neutral oxygen donors. Since comparison is made between two ligands, the different components of energies contributing to the final stability order, shown in Fig. 3.5.11 cancels out. Therefore, Fig. 3.5.12 can be used to predict the expected stability when neutral oxygen donors are added to an existing ligand. In both the relationships shown, minimum strain energy is observed for the large Cs^+ metal ion and maximum strain energy for the small Li^+ ion. Thus, with an increase in metal ion size there is a decrease in the strain energy. The interpretation here is that when neutral

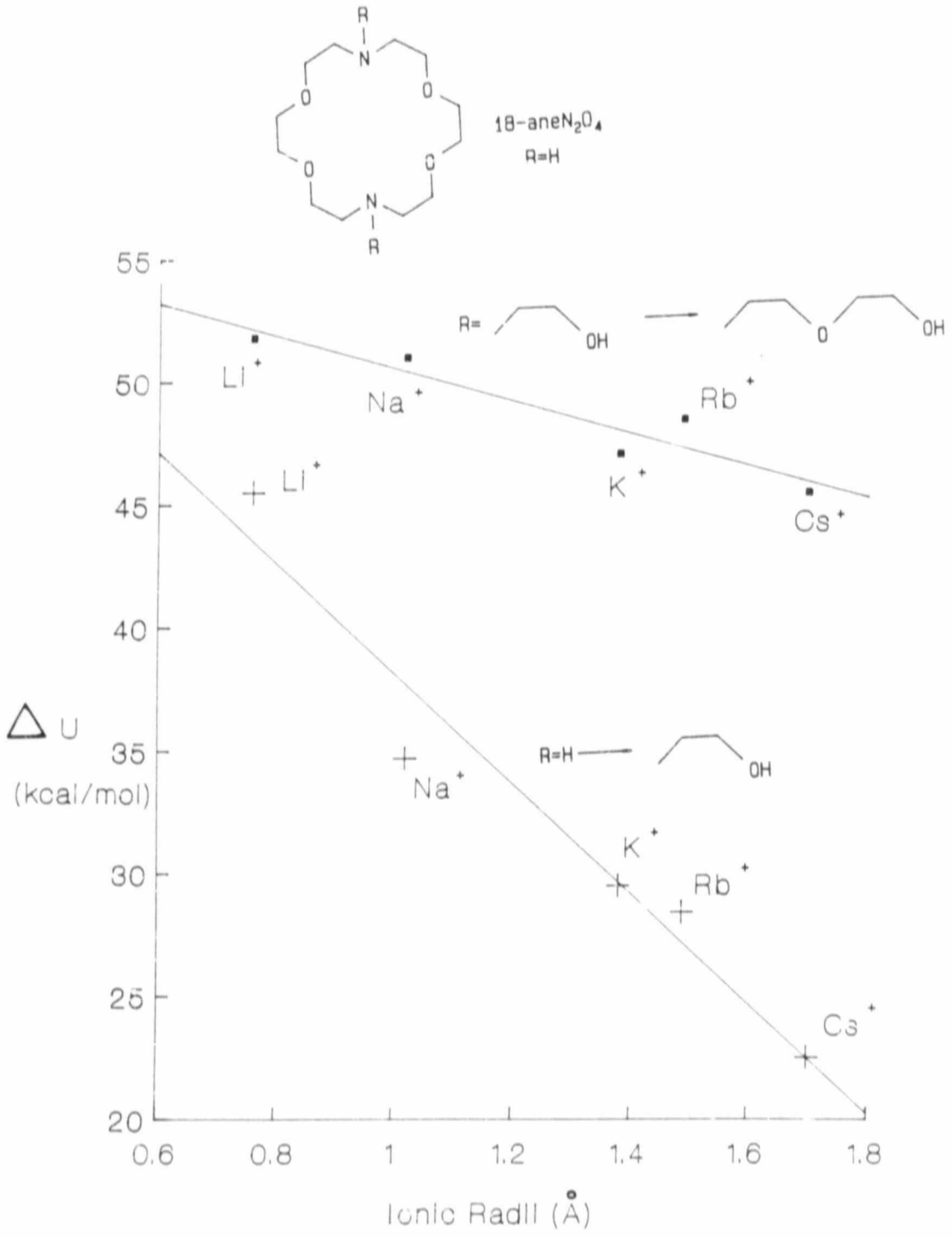

Fig. 3.5.12 The change in total strain energy versus ionic radius for the pair of ligands indicated. Ionic Radii taken from Ref. 98.

oxygen donors are added to an existing ligand, as in BHE–18–aneN_2O_4 and BHEE–18–aneN_2O_4, there is a progressive increase in steric demand. When small metal ions are forced to coordinate to these ligands, the level of steric crowding around the small metal ion increases considerably so that an increase in strain energy is observed. Larger metal ions are still able to accommodate the level of steric crowding required by the ligands BHE–18–aneN_2O_4 and BHEE–18–aneN_2O_4 and so a decrease in strain energy is observed. The metal ions Li^+ and Na^+ will thus form extremely weak complexes with the latter ligands, K^+ a moderately strong complex whereas Rb^+ and Cs^+ should show an increase in complex stability with BHE–18–aneN_2O_4 compared to 18–aneN_2O_4 and a large increase in complex stability with BHEE–18–aneN_2O_4 relative to BHE–18–aneN_2O_4 or 18–aneN_2O_4. The above results are consistent with the complex stabilities reported by Gokel et al. (114) for the pair of ligands 18–aneN_2O_4 and BHE–18–aneN_2O_4. In the case of 18–aneN_2O_4, the K^+ over Na^+ selectivity is –0.24 whereas in BHE–18–aneN_2O_4, which has two more oxygen donors, the K^+ over Na^+ selectivity is 0.21. These results re–emphasize that addition of neutral oxygen donors to existing ligands increases the selectivity of large over small metal ions and that the effect is independent of the type of metal ion.

3.6 MORE RIGID MACROCYCLIC LIGANDS CONTAINING OXYGEN DONORS

An important idea in macrocyclic chemistry has been that of "hole–size–selectivity", that is, the most stable complexes are formed when there is a match between the size of the macrocyclic cavity and the metal ion being complexed. For the series of tetraazamacrocycles 12–aneN_4 to 15–aneN_4, it has been shown (33,37) that the variation in complex stability with a variety of metal ions does not support the idea of "hole–size–selectivity". Instead, the exact opposite to what is expected from "hole–size–selectivity" is observed. Thus, the large metal ion Pb^{2+}

forms the most stable complex with the smallest macrocycle 12–aneN$_4$ whereas the smallest metal ion, low–spin Ni^{2+}, forms the most stable complex with the larger macrocycle, 14–aneN$_4$. The failure to observe this "hole–size–selectivity" is because metal ions are not constrained to coordinate lying in the plane of the macrocycle (24). Thus, smaller macrocycles can accommodate large metal ions by allowing them to coordinate out of the plane of the donor atoms. Coordination of the metal ions in and out of the plane of the macrocycle means that macrocycles are too flexible to display any "hole–size–selectivity". In order to observe genuine "hole–size– selectivity" it is necessary to make the macrocycles more rigid so that metal ions can be forced to coordinate in the plane of the macrocyclic donors. Recently, Hancock et al. (83) have reported a series of rigid macrocyclic ligands which display metal ion size–selectivity. The ligand (1,4–C$_2$)–12–aneN$_4$, shown below, is able to discriminate against large metal ions, as opposed to 12–aneN$_4$ which complexes strongly to large metal ions. On the other extreme is the ligand (C$_2$)$_2$–18–aneN$_4$O$_2$ which coordinates only to the large metal ion Pb^{2+} (83). There are two important features in the latter ligand – a) the presence of the neutral oxygen donor which stabilizes complexes of large metal ions and b) the presence of the piperazine structure, which by molecular mechanics calculations (83) is shown to have the lowest strain energy with large metal ions.

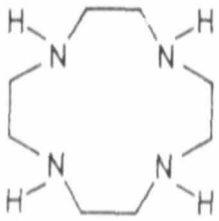

12-aneN$_4$

Prefers large metal ions

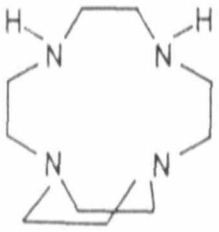

(1, 4-C$_2$) - 12-aneN$_4$

Prefers small metal ions

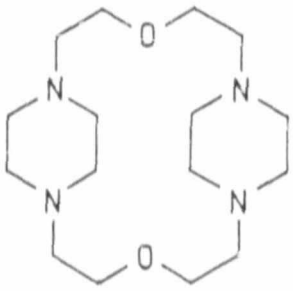

(C$_2$)$_2$-18-aneN$_4$O$_2$

Complexes only to large Pb^{2+}

In order to make the tetraazamacrocycles more rigid, attempts were made to synthesize the ligands I – III shown in Fig. 3.6.1. Present in these structures is the smaller 9–aneN_2O ring which is expected to exhibit rigidity and hence size–selectivity based on the match between cavity size and metal ion size. However, these macrocycles could not be synthesized, although their open–chain analogues were studied. The structures of the open–chain ligands are shown in Fig. 3.6.1 and the protonation and formation constants are given in Table 14. The constants of other similar ligands are given in Table 14 for comparison purposes.

The protonation constants of the aminoalkyl substituted 9–aneN_2O are similar to their open–chain tetraaza amine analogues. The forth protonation constant was too low to have been measured. This could be due to the difficulty in fitting the last proton into the cavity of these ligands, so that the nitrogen is forced to assume an exo conformation, where the nitrogen is orientated outward and the protons directed outside the ligand (125). Increasing the number of methylene bridges, as in going from BAE–9–aneN_2O to BAP–9–aneN_2O or in going from BAE–9–aneN_2O to BAE–10–aneN_2O causes an increase in the basicity of the nitrogen donors. This is expected since BAP–9–aneN_2O and BAE–10–aneN_2O are "longer" amines.

The formation constants of 2,2,2–tet are very similar to BAE–9–aneN_2O. The same type of behaviour is observed for the pair of ligands 3,2,3–tet and BAP–9–aneN_2O. The only metal ion that shows a large increase in going from 2,2,2–tet to BAE–9–aneN_2O is Ni^{2+}. Similar behaviour is observed in going from EN to 9–aneN_2O (38). This is due to the presence of the nine–membered ring, which molecular mechanics calculations (126) have shown to fit best on to small metal ions. The metal ion Cu^{2+} shows a decrease in complex stability in going from 2,2,2–tet to BAE–9–aneN_2O. The reason for this is the preference of Cu^{2+} for square–planar geometry. In BAE–9–aneN_2O the Cu^{2+} is forced to be octahedral and a decrease in stability is observed. The metal ion Zn^{2+} shows an increase in

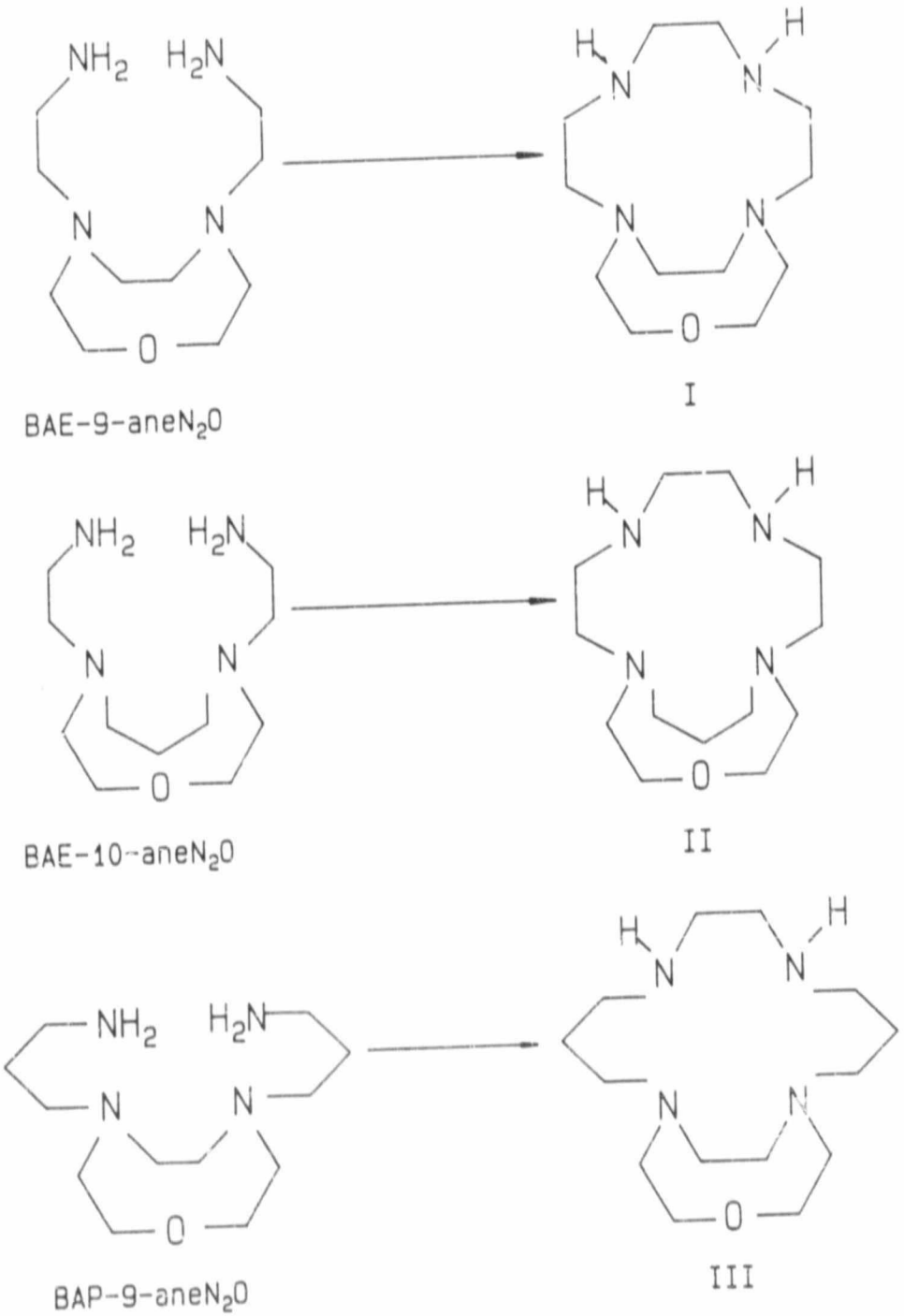

Fig. 3.6.1 Structures of the ligands discussed in this section.

Table 14 Protonation and Formation Constants of some ligands discussed in this work.

	Ionic Radius/Å[a]	BAE–9–aneN$_2$O[b]	BAP–9–aneN$_2$O[b]	BAE–10–ane N$_2$O[b]
pKa_1		9.76(2)	10.36(2)	10.86(2)
pK_2		8.87(2)	9.49(2)	8.91(2)
pKa_3		5.88(2)	7.71(2)	6.90(2)
pKa_4		–	2.14(4)	–
Ni^{2+}[c]	0.7	15.51(5)	14.79(3)	16.51(3)
Cu^{2+}[c]	0.62	19.71(3)	19.00(4)	22.34(3)
Zn^{2+}	0.75	12.66(1)	11.24(1)	12.71(1)
Cd^{2+}	0.95	11.24(1)	8.93(1)	11.73(1)
Pb^{2+}	1.18	10.14(1)	PMH	PMH
		2,2,2–tet[d]	3,2,3–tet[d]	2,3,2–tet[d]
pKa_1		9.74	10.53	9.99
pKa_2		9.08	9.77	9.29
pKa_3		6.56	8.30	7.46
pKa_4		3.24	5.59	5.49
Ni^{2+}		14.0	14.69	16.0
Cu^{2+}		20.1	21.69	23.2
Zn^{2+}		12.03	11.25	12.6
Cd^{2+}		10.62	–	11.1
Pb^{2+}		10.4	–	7.8

[a] Ref 98 [b] This work, 25 °C, 0.1M $NaNO_3$

[c] Equilibrium slow and an out–of–cell titration was followed.

[d] Ref. 20

PMH – precipitation of metal hydroxide

complex stability relative to Pb^{2+} because Zn^{2+} can be better accommodated by the 9–membered ring than Pb^{2+}, and also because of the preference of Zn^{2+} for nitrogen donors.

In Figure 3.6.2a is shown the change in complex stability as a function of metal ion radius as the chelate ring is changed from a five–membered chelate ring to a six–membered chelate ring. It is shown that with an increase in the chelate ring size from a five– to a six–membered ring, there is a steady decrease in complex stability as the metal ion size increases. On the other hand, when two six–membered chelate rings are changed to two five–membered chelate rings, as shown in Fig. 3.6.2b, there is a gradual increase in complex stability with an increase in metal ion size. These results are in accord with the fact that five–membered chelate rings favour the complexation of large metal ions and six–membered chelate rings favour the complexation of small metal ions. Molecular mechanics calculations have demonstrated that the destabilization observed for complexes of small metal ions when a five–membered chelate ring is increased to a six–membered chelate ring is due to steric crowding (34). The response of the metal ion to change in chelate ring size has been interpreted in terms of metal ion size only. Recently, Hancock and Ngwenya (39) have shown that this type of behaviour occurs irrespective of the type of metal ion. Thus Mg^{2+} which has ionic M–L bonding behaved similarly to Cu^{2+} which has more covalent M–L bonding, whereas Cd^{2+} with its covalent M–L bonds behaved similarly to Ca^{2+} which has ionic M–L bonds (39). There is however, a contribution from the oxidation state of the metal ion, such that metal ions of higher oxidation states show a greater decrease in complex stability when there is an increase in chelate ring size, relative to metal ions of the same size but having a lower oxidation state (39). The ability of the larger metal ions to coordinate strongly with five–membered chelate rings derives from the fact that larger metal ions are better suited geometrically to coordinate to the five–membered chelate ring.

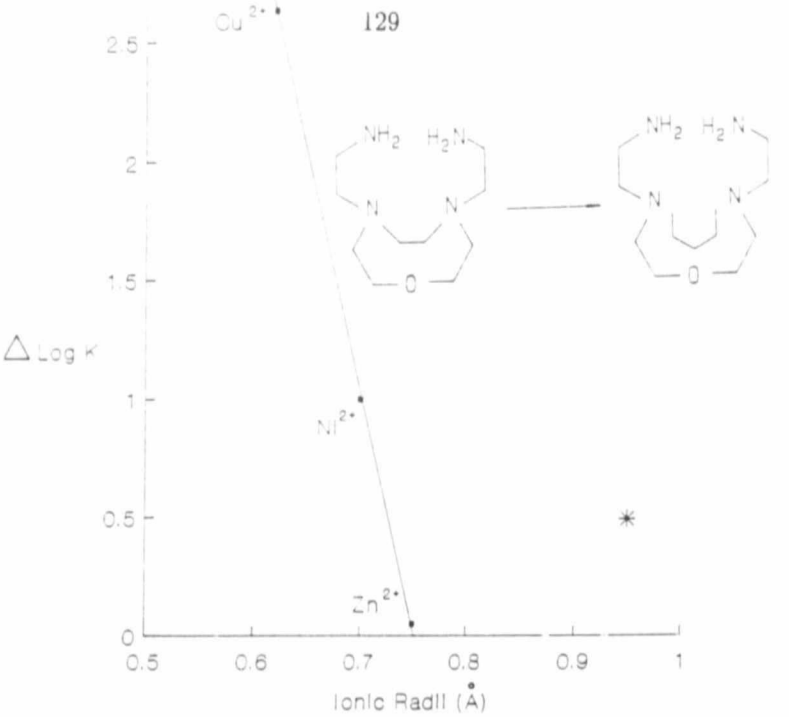

Fig 3.6.2a Change in complex stability, Δ log K, as a function of metal ion radius, in going from BAE–9–aneN_2O to BAE–10–aneN_2O.

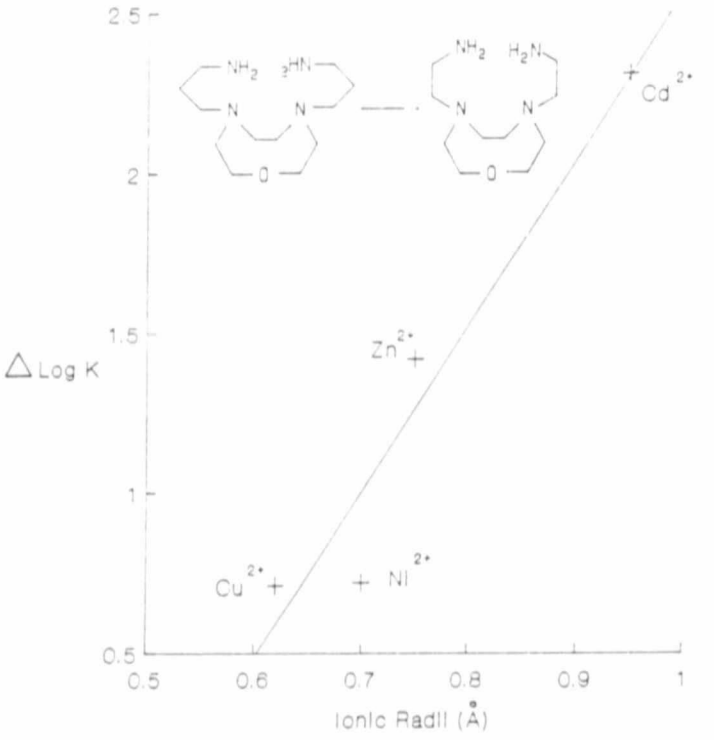

Fig. 3.6.2b Change in complex stability, Δ log K, as a function of metal ion radius, in going from BAP–9–aneN_2O to BAE–9–aneN_2O

Molecular mechanics calculations (9) showed that five–membered chelate rings have minimum strain energy with large M–L bond lengths and small L–M–L angles. Smaller metal ions with their larger L–M–L angles produced a large increase in strain energy. Thus, larger metal ions are able to coordinate with the five–membered chelate ring with less strain energy.

Not much can be discussed about the open chain analogues of the bridged ligands shown in Fig. 3.6.1, except that the stability order follows the "Irving–Williams" series (133) in that $Ni^{2+}<Cu^{2+}>Zn^{2+}$. The need for the synthesis of ligands I – III is thus of importance. These ligands form an interesting trend, in that the cavity sizes follow the order ligand I>II>III. Comparison of the metal binding strengths of these ligands will be of interest since information on size–match selectivity as well as the role of the bridging oxygen donor can be obtained. The magnitude of the macrocyclic effect can also be determined. The latter is particularly important since recent work (83) has shown that in going from BAE–PIP (open–chain analogue of $(1,4–C_2)–12–aneN_4$) to $(1,4–C_2)–12–aneN_4$ there is an increase of 9.6 log units for the Cu^{2+} and Ni^{2+} complexes. This order of magnitude is the largest reported for any macrocyclic systems. In this respect, ligand III should prove to have a high stability for Ni^{2+}. Ligand III is similar to $14–aneN_4$ except for the presence of the bridging ethereal oxygen. The stability constant of Ni^{2+} with $14–aneN_4$ is 20.1 log units (99), whereas with BAP–$9–aneN_2O$, it is 14.79. Ligand III should show an enhanced stability for Ni^{2+} because of the added contribution from the $9–aneN_2O$ type ring incorporated in the structure.